Impacts of Imperfect CSI and Transceiver Hardware Noise on the Performance of Full-Duplex DF Relay System with Multi-Antenna Terminals over Nakagami-m Fading Channels

Ba Cao Nguyen, Le The Dung, *Member, IEEE*, Tran Manh Hoang, Xuan Nam Tran, *Member, IEEE*, Taejoon Kim, *Member, IEEE*

***Abstract*—In this paper, we investigate the performance of a full-duplex (FD) relay system where multi-antennas are exploited at source and destination. Unlike previous works, the impacts of imperfect channel state information (I-CSI), transceiver hardware noise (THN), and residual self-interference (RSI) are taken into account. We mathematically derive the exact closed-form expressions of the outage probability (OP), symbol error rate (SER), and ergodic capacity (EC) of the FD relay system with I-CSI, THN, and RSI over Nakagami-m fading channels. From the derived expressions, the performance of the considered system under the effects of three negative factors (I-CSI, THN, and RSI) is compared with that system in the case of all ideal factors (perfect channel state information (P-CSI), perfect transceiver hardware (P-TH) and perfect self-interference cancellation (P-SIC)), two ideal factors (P-CSI and P-TH, P-CSI and P-SIC, P-TH and P-SIC), or one ideal factor (P-CSI or P-TH or P-SIC). Numerical results show a strong impact of three negative factors on the OP, SER, and EC of the considered FD relay system, especially when the data transmission rate of the system and signal-to-noise ratio (SNR) are high. In particular, OP, SER, and EC go to the floors in the high SNR regime due to the three negative factors. Therefore, when I-CSI, THNs, and RSI exist in the FD relay system, we should use suitable source and relay transmission power to obtain excellent performance while saving energy consumption. Moreover, when two of the three negative factors are large enough, the remaining factor's impact becomes weaker and may be neglected in certain circumstances.**

***Index Terms*—Full-duplex relay, CSI, transceiver hardware noise, self-interference cancellation, outage probability, symbol error rate, ergodic capacity.**

I. Introduction

The fast development of wireless devices, especially for personal users, requires an increase in the capacity of wireless communication systems. Various new technologies such as multiple-input multiple-output (MIMO), full-duplex (FD), cognitive radio (CR), and non-orthogonal multiple access (NOMA) have been proposed to satisfy the capacity requirements of future wireless networks [1]–[4]. Since the MIMO transmission technique can provide high capacity and diversity order, it is not only deployed in the third and fourth generations (3G and 4G) but is also a promising candidate for the fifth-generation (5G) and beyond [5]. However, the hardware deployments and signal processing in MIMO systems, especially the personal devices, are very complex because of multiple radio frequency (RF) signals. Therefore, maximal ratio transmission (MRT) at the transmitter and maximal ratio combining (MRC) at the receiver have been proposed for the MIMO systems to solve these matters [6]. Besides reducing the complexity of MIMO systems, MRT/MRC techniques can significantly improve the system performance by providing the full diversity order. Therefore, applying MRT/MRC techniques in MIMO systems becomes popular in practice.

Recently, FD transmission is exploited in MIMO systems to increase wireless networks' capacity because the FD technique can double spectral efficiency in comparison with the traditional half-duplex (HD) technique. More importantly, besides increasing the capacity, exploiting FD at the relay can improve the coverage and reliability of wireless communication systems [1], [7]. Since a relay is more easily deployed than a base station, it is widely used in wireless systems. Nowadays, FD relay communication systems have been widely investigated in various scenarios, such as in cooperative, energy harvesting (EH), spatial modulation (SM), and CR systems [2], [8], [9]. Their results demonstrated that FD relay systems significantly improve the ergodic capacity (EC) and slightly reduce other performance compared with traditional HD relay systems when all self-interference cancellation (SIC) techniques are effectively applied.

In the literature, besides proposing architectures and algorithms for SIC techniques, investigating the impact of the residual self-interference (RSI) induced by imperfect SIC (I-SIC) on the performance of the FD relay system becomes an attractive issue in both academy and industry. It is because, with the existence of RSI, the system performance in terms of outage probability (OP), symbol error rate (SER) goes to the error floor in the high signal-to-noise ratio (SNR) regime [5], [10]. Also, the power allocation scheme for FD transmission mode significantly reduces the OP and SER of the FD relay system [11]–[13]. Furthermore, the joint impact of RSI and imperfect channel state information (I-CSI) has been considered for FD relay systems [14]–[19]. It was concluded that, under the I-CSI and RSI effects, the OP of the FD relay systems quickly went to the error floor.

As presented in various reports, besides I-CSI, imperfect transceiver hardware or hardware impairment (HI) often occurs in FD relay systems. Although the HI may be known

The work of Taejoon Kim was supported by the Basic Science Research Program through the National Research Foundation of Korea (NRF) funded by the Ministry of Education under Grant 2020R1I1A3068305.

Ba Cao Nguyen is with Chungbuk National University, Cheongju 28644, South Korea and also with Telecommunications University, Khanh Hoa 650000, Vietnam (e-mail: nguyenbacao@tcu.edu.vn).

Le The Dung and Taejoon Kim are with Chungbuk National University, Cheongju 28644, South Korea (e-mails: dung.t.le@ieee.org, ktjcc@chungbuk.ac.kr).

Tran Manh Hoang is with Telecommunications University, Khanh Hoa 650000, Vietnam (e-mail: tranmanhhoang@tcu.edu.vn).

Xuan Nam Tran is with Le Quy Don Technical University, Hanoi 23583, Vietnam (e-mail: namtx@mta.edu.vn).

by the manager and many HI mitigating schemes have been applied at both transmitter and receiver, the HI cannot be completely removed. It is because of the intrinsic properties of electronic components, namely the phase noise and nonlinearities of low-cost oscillators, analog-to-digital (A/D), and digital-to-analog (D/A) converters, mixers, and amplifiers [20], [21]. Furthermore, the HI may come from the imperfect parameter estimation of random and time-varying hardware characteristics, the inaccuracy due to limited precision models, and simple compensation algorithms [20], [22]. The measurements and experiments on the HI after all mitigating solutions demonstrate that residual HI effect on the transceivers can be considered as distortion noise or transceiver hardware noise (THN) [20]–[22].

Initially, the joint impact of THN and CEE on the performance of wireless communication systems with HD relays has often been studied in the literature [23]–[25]. It was demonstrated that the OPs of these HD relay systems reached the ceiling threshold due to the joint impact of THN and CEE. The joint and cross effects of RSI and THN on the OP, SER, and EC of the FD relay systems have considered in recent works [4], [26]. Surprisingly, the impact of THN is more substantial than that of RSI on the OP, SER, and EC of the FD relay systems [4]. In particular, for specific values of RSI, in the case of ideal hardware, the EC of FD relay systems is higher than that of HD relay systems in the low SNR regime but lower in the high SNR regime. However, in the case of THN, the EC of FD relay systems is often higher than that of HD relay systems [4]. On the other hand, the influence of THN is more significant for higher data transmission rate systems. Therefore, in a mathematical analysis, assuming the transceiver to have ideal hardware may result in an inaccurate evaluation of the system performance [27]–[29].

As the above discussions, the joint and cross effects of both I-CSI and RSI, THN, and RSI have been considered in the literature for FD relay systems. However, in practice, FD relay systems are affected not only by two factors, i.e., I-CSI and RSI or THN and RSI, but also by three negative factors, i.e., I-CSI, RSI, and THN. Therefore, neglecting one or two of the three negative factors may lead to underestimating the performance of wireless communication systems. This motivates us to investigate the FD relay system's performance under the joint and cross effects of three negative factors, including I-CSI, THN, and RSI. So far, this is the first work considering the effects of three practical factors (I-CSI, THN, and RSI) on the performance of FD relay system with multi-antenna terminals. Additionally, unlike previous works on FD relay systems, where only one or two metrics were derived, we obtain all important metrics (OP, SER, and EC) to fully evaluate the system performance. The considered FD relay system can be applied to various scenarios requiring massive connections such as cellular systems, low-delay communications, and the 5G heterogeneous networks (HetNets). The main contributions of this paper are summarized as follows:

- We investigate a more realistic FD relay system where I-CSI, THN, and RSI are taken into account for consideration. Notably, the system performance is analyzed over Nakagami-m fading channels because of their generic properties. Thus, we can study this system's performance over other channels such as Rayleigh, Rician, and Gaussian channels.
- We obtain the exact expression of signal-to-interference-plus-noise and distortion ratio (SINDR) and then use it to derive the exact closed-form expressions of OP, SER, and EC of the considered FD relay system under the effects of I-CSI, THN, and RSI. From these expressions, we can quickly obtain the expressions of related systems with P-CSI, P-TH, and P-SIC.
- We analyze the joint and cross impacts of I-CSI, THN, and RSI on the OP, SER, and EC of the considered FD relay system. Various evaluating scenarios are examined to obtain numerical results. The results show that three negative factors have significant effects on the OP, SER, and EC, especially when the transmission rate and SNR are high. Moreover, the OP, SER, and EC with three negative factors are compared with those in the case of all ideal factors, one or two negative factors. When two of the three factors are large enough, the effect of other factors becomes weaker. Some useful recommendations are given to achieve better performance for the considered system.

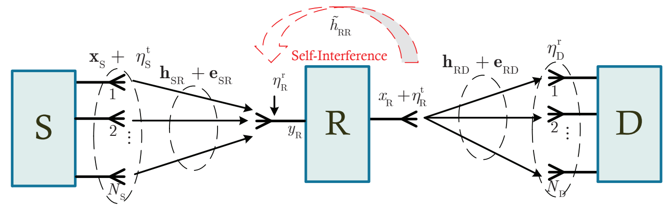

Fig. 1. The block diagram of the considered FD relay system with I-CSI, THN, and RSI.

The rest of this paper is organized as follows. Section II describes the system model, including channel and signal models of the considered FD relay system where the characteristics of I-CSI, THNs, RSI, and the received signals are presented in detail. Section III mathematically derives the expressions of the OP, SER, and EC of the considered system over Nakagami-m fading channels. Numerical results and discussions are given in Section IV. Finally, Section V concludes the paper.

II. System Model

The system model of the considered FD relay system is illustrated in Fig. 1. Signals are transmitted from source (S) to destination (D) via a relay (R) using decode-and-forward (DF) protocol. In the considered system, S and D are equipped with multi-antennas (N_S transmission antennas at S and N_D reception antennas at D) and operate in HD mode. Meanwhile, R operates in FD mode and is equipped with two antennas, one for transmitting and the other for receiving. Due to FD transmission mode, R causes the self-interference (SI) from its transmission antenna to its receiving antenna. Therefore, all SIC techniques such as antenna suppression, analog and digital cancellation should be employed at R to decode the received signals successfully.

A. Channel Model

As shown in Fig. 1, $\mathbf{h}_{\rm SR}$ and $\mathbf{h}_{\rm RD}$ represent the channel vectors of S–R and R–D links, respectively, whose elements follow Nakagami-m distributions. The SI from the transmitting antenna to the receiving antenna of R before applying all SIC techniques is denoted by $\tilde{h}_{\rm RR}$. Due to the far distance and deep fading, the direct link between S and D is neglected.

1) I-CSI Model: Channel estimation is often obtained by using pilot symbols. Before transmitting signals, S/R transmits pilot symbols to R/D, respectively. By monitoring the received signals, the receivers R and D immediately feedback the transmit weights which is used for MRT/MRC techniques at the transmitting antennas and for estimating the instantaneous signal-to-interference-plus-noise-and-distortion ratio (SINDR) at the receiver side. In this paper, we assume that R and D use the minimum-mean-square-error (MMSE) method to estimate the channel vectors of S–R and R–D links [30]. Note that there are many factors that cause the channel estimation errors such as the noise in the received signal, channel frequency offset, Doppler effect, and time synchronization mismatch. To reduce the channel estimation errors, various solutions are applied at the transmitter and receiver such as timing synchronization and cooperative communications [31]. However, it is very challenging to obtain perfect CSI. By using the central limit theorem and experiments, the aggregate effect of these factors can be characterized as a Gaussian distribution.

In the case of I-CSI, the S–R and R–D channels are presented as

$$\hat{\mathbf{h}}_{ij} = \mathbf{h}_{ij} + \mathbf{e}_{ij}, \tag{1}$$

where $ij \in \{\rm SR; RD\}$; $\mathbf{h}_{ij}$ is the channel estimation vector whose elements follow Nakagami-m distributions; $\mathbf{e}_{ij}$ is the channel estimation error vector whose elements follow complex Gaussian distributions with zero means and variances of $\sigma^2_{e_{ij}}$ [15][1].

2) RSI Model: Since FD transmission mode is applied at R, the SIs from transmitting antennas to receiving antennas occur. Furthermore, the distance between the transmission and receiving antennas of R is often very short, the SI power is thus higher than that of the desired signal transmitted from S. Consequently, all SIC techniques including SIC in antenna, analog and digital domains should be exploited at R to mitigate this issue. Generally, R can use a shared-antenna for both transmitting and receiving signals. However, using separate antennas as in this paper can effectively suppress SI, especially in the antenna domain. In addition, the usage of a single antenna for transmitting/receiving at R can significantly reduce the complexity and power consumption. Particularly, in the case that R is equipped with multiple antennas, the signal processing procedures for both self-interference and desired signals are very complex [32], [33]. Thus, it is difficult to suppress the SI effectively with multiple antennas at R. First, various isolation methods such as absorptive shielding, directional isolation, and cross-polarization are applied at R to reduce the SI power [34], [35]. Then, using suitable analog circuits and digital signal processors combined with efficient algorithms can cancel the SI in analog and digital domains. Particularly, R can subtract SI signal from received signals using the digital domain through estimating the SI channel. However, R cannot wholly remove SI because the I-CSI and I-THs induce the SI channel estimation errors [36]. The residual self-interference (RSI) after all SIC solutions still exists in R and reduces the performance and capacity of the considered FD relay system. Fortunately, the SI can be suppressed up to 110 dB, making the RSI power is as low as the noise floor [37]. Additionally, experiments to measure the RSI after all SIC techniques indicated that the RSI follows Gaussian distribution [10], [32], [37][2].

3) Imperfect Transceiver Hardware Model: In practice, wireless devices' hardware is not perfect, making the transmitted and received signals distort. There are various reasons behind the imperfect hardware of wireless systems such as phase noise (PN), in-phase/quadrature (I/Q) imbalance, and nonlinearities of analog-to-digital (A/D), digital-to-analog (D/A) converters, mixers and amplifiers [20]–[22]. Although various techniques such as using stable oscillators, highly linear components, estimation and compensation approaches at both the transmitter and receiver have been applied to deal with the imperfect transceiver hardware [20], [22], the HIs cannot be totally removed. It is because the inaccuracy comes from limited precision models and simple compensation algorithms [20], [38]. On the other hand, the measurements of the residual transceiver hardware impairments indicate that the combined impacts of all impairments at the transmitter and receiver can be considered as a Gaussian random variable with the average noise power is proportional to the average signal power [4], [20]–[22]. Similarly, the effect of the imperfect transceiver hardware in this paper called THN also follows a Gaussian distribution[3]. Additionally, the THNs at the transmitter and the receiver are independent.

As presented in Fig. 1, the THNs at the transmitters S and R are, respectively, denoted by $\boldsymbol{\eta}^{\rm t}_{\rm S}$ and $\eta^{\rm t}_{\rm R}$, where $\boldsymbol{\eta}^{\rm t}_{\rm S} = [\eta^{\rm t}_1\ \eta^{\rm t}_2\ ...\ \eta^{\rm t}_{N_{\rm S}}]^T$. Herein, all elements follow Gaussian distribution, i.e., $\eta^{\rm t}_1 \sim \mathcal{CN}(0, (k^{\rm t}_{\rm S})^2 P_{\rm S}/N_{\rm S})$, $\eta^{\rm t}_{\rm R} \sim \mathcal{CN}(0, (k^{\rm t}_{\rm R})^2 P_{\rm R})$, with $k^{\rm t}_{\rm S}$ and $k^{\rm t}_{\rm R}$, respectively, denote the THN levels at the transmitters S and R; $P_{\rm S}/N_{\rm S}$ and $P_{\rm R}$ are the average

[1]In practice, when the transmission power of S and R increase, the variance of channel estimation error will be reduced. However, it is too difficult to measure the variance of channel estimation error according to the transmission power. Thus, most of works investigating the effect of I-CSI considered it as a constant.

[2]Note that in the literature, the RSI after all SIC techniques is usually characterized as fading model or complex Gaussian random model. In the first model, RSI follows a statistical fading distribution such as Rician/Rayleigh/Nakagami fading. This model often focuses on modeling the self-interference channel. Meanwhile, the second model considers the RSI as a normal random variable to emphasize the impact of the RSI. Although the impact of fading distributed RSI on system performance is similar to that of Gaussian distributed RSI, using fading to model the RSI increases the computational complexity. In our paper, we focus on analyzing the effects of RSI on the system performance. Thus, similar to [5], [8], [36], [37], we assume that the RSI is a complex Gaussian random variable.

[3]As shown in [20]–[22], the residual impairments are caused by the intrinsic defects of electronic components, the random and time varying hardware characteristics, the inaccuracy coming from limited precision models, unsophisticated compensation algorithms, etc. Importantly, all impairments are time-dependent because they take new realizations for each new data signal [20]. Based on central limit theorem and experiments, the complex Gaussian variables are accurate for modeling the aggregate effect of many impairments.

transmission power per one antenna of S and R, respectively. The THNs at the receivers R and D are, respectively, denoted by $\eta_{\mathrm{R}}^{\mathrm{r}}$ and $\boldsymbol{\eta}_{\mathrm{D}}^{\mathrm{r}}$, where $\eta_{\mathrm{R}}^{\mathrm{r}} \sim \mathcal{CN}(0, \|\hat{\mathbf{h}}_{\mathrm{SR}}\|^2 (k_{\mathrm{R}}^{\mathrm{r}})^2 \frac{P_{\mathrm{S}}}{N_{\mathrm{S}}})$, $\boldsymbol{\eta}_{\mathrm{D}}^{\mathrm{r}} = [\eta_1^{\mathrm{r}}\ \eta_2^{\mathrm{r}}\ ...\ \eta_{N_{\mathrm{D}}}^{\mathrm{r}}]^T$. Herein, all elements follow Gaussian distribution, i.e., $\eta_1^{\mathrm{r}} \sim \mathcal{CN}(0, \|\hat{\mathbf{h}}_{\mathrm{RD}}\|^2 (k_{\mathrm{D}}^{\mathrm{r}})^2 P_{\mathrm{R}})$, with $k_{\mathrm{R}}^{\mathrm{r}}$ and $k_{\mathrm{D}}^{\mathrm{r}}$ denote the THN levels at the receivers R and D, respectively.

B. Signal Model

From the previous channel model, we formulate the received signals at the receivers R and D, then derive the SINDR expressions at these two receivers for further analysis.

The received signals at R is computed as

$$y_{\mathrm{R}} = \hat{\mathbf{h}}_{\mathrm{SR}}^H (\mathbf{x}_{\mathrm{S}} + \boldsymbol{\eta}_{\mathrm{S}}^{\mathrm{t}}) + \eta_{\mathrm{R}}^{\mathrm{r}} + \tilde{h}_{\mathrm{RR}}(x_{\mathrm{R}} + \eta_{\mathrm{R}}^{\mathrm{t}}) + \tilde{\eta}_{\mathrm{R}}^{\mathrm{r}} + z_{\mathrm{R}}, \quad (2)$$

where $\hat{\mathbf{h}}_{\mathrm{SR}}^H = [\hat{h}_{1\mathrm{R}}\ \hat{h}_{2\mathrm{R}}\ ...\ \hat{h}_{N_{\mathrm{S}}\mathrm{R}}]$ is the channel vector from N_{S} transmitting antennas of S to the receiving antenna of R; $\mathbf{x}_{\mathrm{S}} = [x_1\ x_2\ ...\ x_{N_{\mathrm{S}}}]^{T}$[4] is the intended signal vector from N_{S} transmitting antennas of S; $\boldsymbol{\eta}_{\mathrm{S}}^{\mathrm{t}} = [\eta_1^{\mathrm{t}}\ \eta_2^{\mathrm{t}}\ ...\ \eta_{N_{\mathrm{S}}}^{\mathrm{t}}]^T$ is the THN vector caused by transmitter S; $\eta_{\mathrm{R}}^{\mathrm{r}}$ is the THN caused by receiver R for S–R channel; $\tilde{h}_{\mathrm{RR}}$ is the SI channel caused by FD transmission mode from transmission to receiving antennas of R; x_{R} is intended transmitted signal at R; $\eta_{\mathrm{R}}^{\mathrm{t}}$ is the THN caused by transmitter R; $\tilde{\eta}_{\mathrm{R}}^{\mathrm{r}}$ is the THN caused by the receiver R for SI channel; z_{R} is Gaussian noise at R which has zero mean and variance of σ_{R}^2, i.e., $z_{\mathrm{R}} \sim \mathcal{CN}(0, \sigma_{\mathrm{R}}^2)$.

As can be seen from (2), there are three terms in the received signal of R, i.e., the intended signal and THN of S–R channel ($\hat{\mathbf{h}}_{\mathrm{SR}}^H (\mathbf{x}_{\mathrm{S}} + \boldsymbol{\eta}_{\mathrm{S}}^{\mathrm{t}}) + \eta_{\mathrm{R}}^{\mathrm{r}}$), the SI signal and THN of SI channel ($\tilde{h}_{\mathrm{RR}}(x_{\mathrm{R}} + \eta_{\mathrm{R}}^{\mathrm{t}}) + \tilde{\eta}_{\mathrm{R}}^{\mathrm{r}} = \tilde{h}_{\mathrm{RR}} x_{\mathrm{R}} + \tilde{h}_{\mathrm{RR}} \eta_{\mathrm{R}}^{\mathrm{t}} + \tilde{\eta}_{\mathrm{R}}^{\mathrm{r}}$), and Gaussian noise ($z_{\mathrm{R}}$). For FD relay, since the distance between transmitting and receiving antennas of R is very small, especially for personal devices[5], the power of SI signal ($\tilde{h}_{\mathrm{RR}} x_{\mathrm{R}}$) is much higher than that of THN ($\tilde{h}_{\mathrm{RR}} \eta_{\mathrm{R}}^{\mathrm{t}} + \tilde{\eta}_{\mathrm{R}}^{\mathrm{r}}$). Thus, the SI and THN of the SI channel can be approximated as $\tilde{h}_{\mathrm{RR}}(x_{\mathrm{R}} + \eta_{\mathrm{R}}^{\mathrm{t}}) + \tilde{\eta}_{\mathrm{R}}^{\mathrm{r}} \approx \tilde{h}_{\mathrm{RR}} x_{\mathrm{R}}$. After receiving signal, R applies all SIC techniques in antenna, analog and digital domains as presented above to reduce the SI power. Then, the RSI at R (denoted by I_{R}) is Gaussian distributed, i.e., $I_{\mathrm{R}} \sim \mathcal{CN}(0, l^2 P_{\mathrm{R}})$, where l denotes the RSI level at R [36], [37].

Now, (2) becomes

$$y_{\mathrm{R}} = \hat{\mathbf{h}}_{\mathrm{SR}}^H (\mathbf{x}_{\mathrm{S}} + \boldsymbol{\eta}_{\mathrm{S}}^{\mathrm{t}}) + \eta_{\mathrm{R}}^{\mathrm{r}} + I_{\mathrm{R}} + z_{\mathrm{R}}. \quad (3)$$

Using (1), (3) can be rewritten as

$$y_{\mathrm{R}} = \mathbf{h}_{\mathrm{SR}} \mathbf{x}_{\mathrm{S}} + \mathbf{h}_{\mathrm{SR}} \boldsymbol{\eta}_{\mathrm{S}}^{\mathrm{t}} + \eta_{\mathrm{R}}^{\mathrm{r}} + \mathbf{e}_{\mathrm{SR}} \mathbf{x}_{\mathrm{S}} + \mathbf{e}_{\mathrm{SR}} \boldsymbol{\eta}_{\mathrm{S}}^{\mathrm{t}} + I_{\mathrm{R}} + z_{\mathrm{R}}. \quad (4)$$

As can be seen from (4), the received signals at R include six terms, i.e., desired signal ($\mathbf{h}_{\mathrm{SR}} \mathbf{x}_{\mathrm{S}}$), THN ($\mathbf{h}_{\mathrm{SR}} \boldsymbol{\eta}_{\mathrm{S}}^{\mathrm{t}} + \eta_{\mathrm{R}}^{\mathrm{r}}$), channel estimation error (CEE) ($\mathbf{e}_{\mathrm{SR}} \mathbf{x}_{\mathrm{S}}$), product of CEE and THN ($\mathbf{e}_{\mathrm{SR}} \boldsymbol{\eta}_{\mathrm{S}}^{\mathrm{t}}$), RSI ($I_{\mathrm{R}}$), and Gaussian noise ($z_{\mathrm{R}}$). However, they can be classified in two groups, i.e., desired signal ($\mathbf{h}_{\mathrm{SR}} \mathbf{x}_{\mathrm{S}}$) and undesired signals ($\mathbf{h}_{\mathrm{SR}} \boldsymbol{\eta}_{\mathrm{S}}^{\mathrm{t}} + \eta_{\mathrm{R}}^{\mathrm{r}}$, $\mathbf{e}_{\mathrm{SR}} \mathbf{x}_{\mathrm{S}}$, $\mathbf{e}_{\mathrm{SR}} \boldsymbol{\eta}_{\mathrm{S}}^{\mathrm{t}}$, I_{R}, and z_{R}). As demonstrated in the literature [22], [43], [44], although the received signal may contain many variables and multiplications of some variables, the SINDR is still calculated by dividing the desired signal power by the undesired signal power (i.e., the interference-plus-noise-and-distortion power).

From (4), the SINDR at R (denoted by γ_{R}) for detecting the intended signal is calculated as (5) on the next page, where $k_{\mathrm{SR}}^2 = (k_{\mathrm{S}}^{\mathrm{t}})^2 + (k_{\mathrm{R}}^{\mathrm{r}})^2$ is the aggregated THN level combined from the transmitter S ($k_{\mathrm{S}}^{\mathrm{t}}$) and the receiver R ($k_{\mathrm{R}}^{\mathrm{r}}$)[6].

After decoding the received signals, R re-encodes and forwards them to D. The received signals at D is

$$\mathbf{y}_{\mathrm{D}} = \hat{\mathbf{h}}_{\mathrm{RD}}(x_{\mathrm{R}} + \eta_{\mathrm{R}}^{\mathrm{t}}) + \boldsymbol{\eta}_{\mathrm{D}}^{\mathrm{r}} + \mathbf{z}_{\mathrm{D}}, \quad (6)$$

where $\hat{\mathbf{h}}_{\mathrm{RD}} = [\hat{h}_{\mathrm{R}1}\ \hat{h}_{\mathrm{R}2}\ ...\ \hat{h}_{\mathrm{R}N_{\mathrm{D}}}]^T$ is the channel vector from the transmitting antenna of R to N_{D} receiving antennas of D; $\boldsymbol{\eta}_{\mathrm{D}}^{\mathrm{r}} = [\eta_1^{\mathrm{r}}\ \eta_2^{\mathrm{r}}\ ...\ \eta_{N_{\mathrm{D}}}^{\mathrm{r}}]^T$ is the THN vector at D; $\mathbf{z}_{\mathrm{D}}$ is the noise vector at D, whose each element follows Gaussian distribution with zero mean and variance of σ_{D}^2.

Substituting (1) into (6), we have

$$\mathbf{y}_{\mathrm{D}} = \mathbf{h}_{\mathrm{RD}} x_{\mathrm{R}} + \mathbf{h}_{\mathrm{RD}} \eta_{\mathrm{R}}^{\mathrm{t}} + \boldsymbol{\eta}_{\mathrm{D}}^{\mathrm{r}} + \mathbf{e}_{\mathrm{RD}} x_{\mathrm{R}} + \mathbf{e}_{\mathrm{RD}} \eta_{\mathrm{R}}^{\mathrm{t}} + \mathbf{z}_{\mathrm{D}}. \quad (7)$$

From (7), the SINDR at D (denoted by γ_{D}) is expressed as (8) on the next page, where $k_{\mathrm{RD}}^2 = (k_{\mathrm{R}}^{\mathrm{t}})^2 + (k_{\mathrm{D}}^{\mathrm{r}})^2$ denotes the aggregated THN level at both transmitter R ($k_{\mathrm{R}}^{\mathrm{t}}$) and receiver D ($k_{\mathrm{D}}^{\mathrm{r}}$).

Since DF protocol is applied at FD relay, the end-to-end SINDR (denoted by γ_{e2e}) of the considered FD relay system is computed as [43]

$$\gamma_{\mathrm{e2e}} = \min\{\gamma_{\mathrm{R}}, \gamma_{\mathrm{D}}\}, \quad (9)$$

where γ_{R} and γ_{D} are given in (5) and (8), respectively.

III. Performance Analysis

A. Outage Probability

The OP is a vital evaluation metric of the wireless systems and often needs to be obtained first. Besides being used for indicating whether the instantaneous data transmission rate of a wireless system satisfies a predefined data transmission rate or not, the OP can be used in calculating other metrics such as SER and EC. Especially when it is very challenging to compute the SER, the diversity order of the wireless system can be directly determined from the OP.

Mathematically, the OP of the considered FD relay system (denoted by $\mathcal{P}_{\mathrm{out}}$) can be calculated as [45]

$$\mathcal{P}_{\mathrm{out}} = \Pr\{\log_2(1 + \gamma_{\mathrm{e2e}}) < \mathcal{R}\}, \quad (10)$$

where γ_{e2e} and $\mathcal{R}$ are the end-to-end SINDR and the pre-data transmission rate of the considered system, respectively.

[4]Notice that $(.)^T$ and $(.)^H$ denote the transpose and conjugate-transpose of a vector or matrix, respectively.

[5]Recently, a personal device often acts as an FD relay when it is exploited in non-orthogonal multiple access (NOMA) systems [39]–[41]. In this case, a personal device is a near user receiving both its signal and a far user's signal. After decoding or amplifying these signals, the near user forwards them to the far user. In another case, a personal device serves as an FD relay for different data flows in decentralized ad-hoc wireless networks [42].

[6]Note that for the received signal in (4), the SINDR expression given in (5) is applied for all kinds of channel distributions including Rayleigh, Rician, and Nakagami. The channel distributions only influence the calculations of the OP and the cumulative distribution function, but not the SINDR.

$$\begin{aligned}\gamma_{\mathrm{R}} &= \frac{\|\mathbf{h}_{\mathrm{SR}}\|^2 \frac{P_{\mathrm{S}}}{N_{\mathrm{S}}}}{\|\mathbf{h}_{\mathrm{SR}}\|^2 (k_{\mathrm{S}}^{\mathrm{t}})^2 \frac{P_{\mathrm{S}}}{N_{\mathrm{S}}} + \|\hat{\mathbf{h}}_{\mathrm{SR}}\|^2 (k_{\mathrm{R}}^{\mathrm{r}})^2 \frac{P_{\mathrm{S}}}{N_{\mathrm{S}}} + \sigma_{e_{\mathrm{SR}}}^2 \frac{P_{\mathrm{S}}}{N_{\mathrm{S}}} + \sigma_{e_{\mathrm{SR}}}^2 (k_{\mathrm{S}}^{\mathrm{t}})^2 \frac{P_{\mathrm{S}}}{N_{\mathrm{S}}} + l^2 P_{\mathrm{R}} + \sigma_{\mathrm{R}}^2} \\ &= \frac{\|\mathbf{h}_{\mathrm{SR}}\|^2 \frac{P_{\mathrm{S}}}{N_{\mathrm{S}}}}{\|\mathbf{h}_{\mathrm{SR}}\|^2 (k_{\mathrm{S}}^{\mathrm{t}})^2 \frac{P_{\mathrm{S}}}{N_{\mathrm{S}}} + \|\mathbf{h}_{\mathrm{SR}}\|^2 (k_{\mathrm{R}}^{\mathrm{r}})^2 \frac{P_{\mathrm{S}}}{N_{\mathrm{S}}} + \sigma_{e_{\mathrm{SR}}}^2 (k_{\mathrm{R}}^{\mathrm{r}})^2 \frac{P_{\mathrm{S}}}{N_{\mathrm{S}}} + \sigma_{e_{\mathrm{SR}}}^2 \frac{P_{\mathrm{S}}}{N_{\mathrm{S}}} + \sigma_{e_{\mathrm{SR}}}^2 (k_{\mathrm{S}}^{\mathrm{t}})^2 \frac{P_{\mathrm{S}}}{N_{\mathrm{S}}} + l^2 P_{\mathrm{R}} + \sigma_{\mathrm{R}}^2} \\ &= \frac{\|\mathbf{h}_{\mathrm{SR}}\|^2 P_{\mathrm{S}}}{\|\mathbf{h}_{\mathrm{SR}}\|^2 k_{\mathrm{SR}}^2 P_{\mathrm{S}} + \sigma_{e_{\mathrm{SR}}}^2 P_{\mathrm{S}} (1 + k_{\mathrm{SR}}^2) + N_{\mathrm{S}} (l^2 P_{\mathrm{R}} + \sigma_{\mathrm{R}}^2)}, \end{aligned} \tag{5}$$

$$\begin{aligned}\gamma_{\mathrm{D}} &= \frac{\|\mathbf{h}_{\mathrm{RD}}\|^2 P_{\mathrm{R}}}{\|\mathbf{h}_{\mathrm{RD}}\|^2 (k_{\mathrm{R}}^{\mathrm{t}})^2 P_{\mathrm{R}} + \|\hat{\mathbf{h}}_{\mathrm{RD}}\|^2 (k_{\mathrm{D}}^{\mathrm{r}})^2 P_{\mathrm{R}} + \sigma_{e_{\mathrm{SR}}}^2 P_{\mathrm{R}} + \sigma_{e_{\mathrm{SR}}}^2 (k_{\mathrm{R}}^{\mathrm{t}})^2 P_{\mathrm{R}} + \sigma_{\mathrm{D}}^2} \\ &= \frac{\|\mathbf{h}_{\mathrm{RD}}\|^2 P_{\mathrm{R}}}{\|\mathbf{h}_{\mathrm{RD}}\|^2 (k_{\mathrm{R}}^{\mathrm{t}})^2 P_{\mathrm{R}} + \|\mathbf{h}_{\mathrm{RD}}\|^2 (k_{\mathrm{D}}^{\mathrm{r}})^2 P_{\mathrm{R}} + \sigma_{e_{\mathrm{SR}}}^2 (k_{\mathrm{D}}^{\mathrm{r}})^2 P_{\mathrm{R}} + \sigma_{e_{\mathrm{SR}}}^2 P_{\mathrm{R}} + \sigma_{e_{\mathrm{SR}}}^2 (k_{\mathrm{R}}^{\mathrm{t}})^2 P_{\mathrm{R}} + \sigma_{\mathrm{D}}^2} \\ &= \frac{\|\mathbf{h}_{\mathrm{RD}}\|^2 P_{\mathrm{R}}}{\|\mathbf{h}_{\mathrm{RD}}\|^2 k_{\mathrm{RD}}^2 P_{\mathrm{R}} + \sigma_{e_{\mathrm{SR}}}^2 P_{\mathrm{R}} (1 + k_{\mathrm{RD}}^2) + \sigma_{\mathrm{D}}^2}, \end{aligned} \tag{8}$$

Now, we rewrite (10) as

$$\mathcal{P}_{\mathrm{out}} = \Pr\{\gamma_{\mathrm{e2e}} < 2^{\mathcal{R}} - 1\}. \tag{11}$$

By changing variable, i.e., $\gamma_{\mathrm{th}} = 2^{\mathcal{R}} - 1$, where γ_{th} is called as the SINDR threshold, then (11) becomes

$$\begin{aligned}\mathcal{P}_{\mathrm{out}} &= \Pr\{\gamma_{\mathrm{e2e}} < \gamma_{\mathrm{th}}\} = \Pr\{\min\{\gamma_{\mathrm{R}}, \gamma_{\mathrm{D}}\} < \gamma_{\mathrm{th}}\} \\ &= \Pr\{\gamma_{\mathrm{R}} < \gamma_{\mathrm{th}}\} + \Pr\{\gamma_{\mathrm{D}} < \gamma_{\mathrm{th}}\} \\ &\quad - \Pr\{(\gamma_{\mathrm{R}} < \gamma_{\mathrm{th}}) \cap (\gamma_{\mathrm{D}} < \gamma_{\mathrm{th}})\}. \end{aligned} \tag{12}$$

Since $\gamma_{\mathrm{R}} < \gamma_{\mathrm{th}}$ and $\gamma_{\mathrm{D}} < \gamma_{\mathrm{th}}$ are two independent events, (12) can be expressed as

$$\begin{aligned}\mathcal{P}_{\mathrm{out}} &= \Pr\{\gamma_{\mathrm{R}} < \gamma_{\mathrm{th}}\} + \Pr\{\gamma_{\mathrm{D}} < \gamma_{\mathrm{th}}\} \\ &\quad - \Pr\{\gamma_{\mathrm{R}} < \gamma_{\mathrm{th}}\} \Pr\{\gamma_{\mathrm{D}} < \gamma_{\mathrm{th}}\}. \end{aligned} \tag{13}$$

From (13), the OP of the considered FD relay system is derived in the following Theorem 1.

Theorem 1. *The OP of the considered FD relay system under the effect of I-CSI, THN, and RSI over Nakagami-m fading channels is computed as*

$$\mathcal{P}_{\mathrm{out}} = \begin{cases} 1 - \exp\left(-\frac{\gamma_{\mathrm{th}} A}{1 - \gamma_{\mathrm{th}} k_{\mathrm{SR}}^2} - \frac{\gamma_{\mathrm{th}} B}{1 - \gamma_{\mathrm{th}} k_{\mathrm{RD}}^2}\right) \sum\limits_{i=0}^{m_1 N_{\mathrm{S}} - 1} \sum\limits_{j=0}^{m_2 N_{\mathrm{D}} - 1} \\ \times \frac{1}{i! j!} \left(\frac{\gamma_{\mathrm{th}} A}{1 - \gamma_{\mathrm{th}} k_{\mathrm{SR}}^2}\right)^i \left(\frac{\gamma_{\mathrm{th}} B}{1 - \gamma_{\mathrm{th}} k_{\mathrm{RD}}^2}\right)^j, \gamma_{\mathrm{th}} < 1/\Delta^2 \\ 1, \gamma_{\mathrm{th}} \geq 1/\Delta^2 \end{cases} \tag{14}$$

where $A = \frac{m_1[\sigma_{e_{\mathrm{SR}}}^2 P_{\mathrm{S}}(1 + k_{\mathrm{SR}}^2) + N_{\mathrm{S}}(l^2 P_{\mathrm{R}} + \sigma_{\mathrm{R}}^2)]}{\Omega_{\mathrm{SR}} P_{\mathrm{S}}}$, $B = \frac{m_2[\sigma_{e_{\mathrm{RD}}}^2 P_{\mathrm{R}}(1 + k_{\mathrm{RD}}^2) + \sigma_{\mathrm{D}}^2]}{\Omega_{\mathrm{RD}} P_{\mathrm{R}}}$, m_1 *and* $\Omega_{\mathrm{SR}} = \mathbb{E}\{h_{1\mathrm{R}}\} = \mathbb{E}\{h_{2\mathrm{R}}\} = \ldots = \mathbb{E}\{h_{\mathrm{N_S R}}\}$ *are, respectively, the Nakagami parameter and the average channel gain of S–R communication link,* m_2 *and* $\Omega_{\mathrm{RD}} = \mathbb{E}\{h_{\mathrm{R}1}\} = \mathbb{E}\{h_{\mathrm{R}2}\} = \ldots = \mathbb{E}\{h_{\mathrm{RN_D}}\}$ *are respectively the Nakagami parameter and the average channel gain of R–D communication link,* $\Delta = \max\{k_{\mathrm{SR}}, k_{\mathrm{RD}}\}$.

Proof: The detailed proof is presented in Appendix A.

Remark: To get more insights into the impacts of system parameters on the performance of the FD relay system, we derive the asymptotic expression of the OP when the transmission power is extremely large. In particular, we set $P_{\mathrm{S}} = P_{\mathrm{R}} = P$, $\Omega_{\mathrm{SR}} = \Omega_{\mathrm{RD}} = \Omega$, $m_1 = m_2 = m$, $\sigma_{e_{\mathrm{SR}}}^2 = \sigma_{e_{\mathrm{RD}}}^2 = \sigma_e^2$, $k_{\mathrm{S}}^{\mathrm{t}} = k_{\mathrm{R}}^{\mathrm{r}} = k_{\mathrm{R}}^{\mathrm{t}} = k_{\mathrm{D}}^{\mathrm{r}} = k$, $\sigma_{\mathrm{R}}^2 = \sigma_{\mathrm{D}}^2 = \sigma^2$, $N_{\mathrm{S}} = N_{\mathrm{D}} = N$, and SNR = P/σ^2. These assumptions lead to $k_{\mathrm{SR}} = k_{\mathrm{RD}} = \Delta$ and the terms A and B in Theorem 1 are now, respectively, given by

$$A = \frac{m[\sigma_e^2 \mathrm{SNR}(1 + \Delta^2) + N(l^2 \mathrm{SNR} + 1)]}{\Omega \mathrm{SNR}}, \tag{15}$$

$$B = \frac{m[\sigma_e^2 \mathrm{SNR}(1 + \Delta^2) + 1]}{\Omega \mathrm{SNR}}. \tag{16}$$

Additionally, applying the approximation of exponential function, i.e., $\exp(-x) \approx 1 - x$, the OP expression in the case $\gamma_{\mathrm{th}} < 1/\Delta^2$ becomes

$$\begin{aligned}\mathcal{P}_{\mathrm{out}} &\approx 1 - \left(1 - \frac{\gamma_{\mathrm{th}} A}{1 - \gamma_{\mathrm{th}} \Delta^2} - \frac{\gamma_{\mathrm{th}} B}{1 - \gamma_{\mathrm{th}} \Delta^2}\right) \\ &\quad \times \sum_{i=0}^{mN-1} \sum_{j=0}^{mN-1} \frac{1}{i! j!} \left(\frac{\gamma_{\mathrm{th}} A}{1 - \gamma_{\mathrm{th}} \Delta^2}\right)^i \left(\frac{\gamma_{\mathrm{th}} B}{1 - \gamma_{\mathrm{th}} \Delta^2}\right)^j \\ &= 1 - \left[1 - \frac{\gamma_{\mathrm{th}}}{1 - \gamma_{\mathrm{th}} \Delta^2} (A + B)\right] \\ &\quad \times \sum_{i=0}^{mN-1} \sum_{j=0}^{mN-1} \frac{1}{i! j!} \left(\frac{\gamma_{\mathrm{th}}}{1 - \gamma_{\mathrm{th}} \Delta^2}\right)^{i+j} A^i B^j. \end{aligned} \tag{17}$$

When the transmission power is extremely large, i.e., $\mathrm{SNR} \to \infty$, we have

$$\lim_{\mathrm{SNR} \to \infty} A = \frac{m[\sigma_e^2 (1 + \Delta^2) + N l^2]}{\Omega}, \tag{18}$$

$$\lim_{\mathrm{SNR} \to \infty} B = \frac{m \sigma_e^2 (1 + \Delta^2)}{\Omega}. \tag{19}$$

Therefore, in high SNR regime, we can present the OP in the case $\gamma_{\rm th} < 1/\Delta^2$ as

$$\lim_{\mathrm{SNR}\to\infty} \mathcal{P}_{\rm out} = 1 - \Big[1 - \frac{\gamma_{\rm th}}{1-\gamma_{\rm th}\Delta^2}\Big(\frac{2m\sigma_e^2(1+\Delta^2)+Nl^2}{\Omega}\Big)\Big] \times \sum_{i=0}^{mN-1}\sum_{j=0}^{mN-1}\frac{1}{i!j!}\Big(\frac{\gamma_{\rm th}}{1-\gamma_{\rm th}\Delta^2}\Big)^{i+j} \times \Big(\frac{m[\sigma_e^2(1+\Delta^2)+Nl^2]}{\Omega}\Big)^i\Big(\frac{m\sigma_e^2(1+\Delta^2)}{\Omega}\Big)^j. \tag{20}$$

As shown in (20), the value of $\mathcal{P}_{\rm out}$ in high SNR regime depends on the average channel gain (Ω), the Nakagami-m fading parameter (m), the variance of channel estimation error (σ_e^2), the THN level (Δ), the RSI level (l), the threshold ($\gamma_{\rm th}$), and the number of transmitting antennas at S and receiving antennas at D (N). Since Ω, m, σ_e^2, Δ, l, $\gamma_{\rm th}$, and N are constants, the value of $\mathcal{P}_{\rm out}$ in high SNR regime is a constant. In other words, the joint impacts of I-CSI, THN and RSI cause the error floor of the OP of the considered FD relay system.

B. Symbol Error Rate

The SER is used to investigate if a system can or cannot satisfy the requirements of the error when being used in practice. Mathematically, the SER of the considered FD relay system can be calculated as [45]

$$\mathrm{SER} = \alpha\mathbb{E}\{Q(\sqrt{\beta\gamma_{\rm e2e}})\} = \frac{\alpha}{\sqrt{2\pi}}\int_0^\infty F\Big(\frac{t^2}{\beta}\Big)\exp\Big(-\frac{t^2}{2}\Big)dt, \tag{21}$$

where (α,β) is a modulation couple whose values are obtained from certain modulation types, e.g., $(\alpha,\beta)=(1,2)$ and $(\alpha,\beta)=(2,1)$ for the binary phase-shift keying (BPSK) modulation and the 4-quadrature amplitude modulation (4-QAM), respectively; $Q(.)$ denotes the Gaussian function; $\gamma_{\rm e2e}$ and $F(.)$ are respectively the end-to-end SINDR and its cumulative distribution function (CDF). By changing variable, i.e., $x = t^2/\beta$, (21) becomes

$$\mathrm{SER} = \frac{\alpha\sqrt{\beta}}{2\sqrt{2\pi}}\int_0^\infty \frac{\exp\Big(-\frac{x\beta}{2}\Big)}{\sqrt{x}}F(x)dx. \tag{22}$$

From (22), the SER of the considered FD relay system is computed in the following Theorem 2.

Theorem 2. *Under the impacts of I-CSI, THN, and RSI, the SER of the considered FD relay system over Nakagami-m fading channels is given as*

$$\mathrm{SER} = \frac{\alpha\sqrt{\beta}}{2\sqrt{2\pi}}\Bigg[\sqrt{\frac{2\pi}{\beta}} - \frac{\pi}{\sqrt{2}G\Delta}\sum_{g=1}^{G}\sum_{i=0}^{m_1N_{\rm S}-1}\sum_{j=0}^{m_2N_{\rm D}-1} \times \frac{A^iB^j\sqrt{1-\phi_g^2}(1+\phi_g)^{i+j-\frac{1}{2}}}{i!j!\Big(2\Delta^2-(1+\phi_g)k_{\rm SR}^2\Big)^i\Big(2\Delta^2-(1+\phi_g)k_{\rm RD}^2\Big)^j} \exp\Big(-\frac{(1+\phi_g)A}{2\Delta^2-(1+\phi_g)k_{\rm SR}^2} - \frac{(1+\phi_g)B}{2\Delta^2-(1+\phi_g)k_{\rm RD}^2}\Big)\Bigg], \tag{23}$$

where G is the complexity-accuracy trade-off parameter; $\phi_g = \cos\Big(\frac{(2g-1)\pi}{2G}\Big)$.

Proof: Detailed proof is presented in Appendix B.

C. Ergodic Capacity

The EC of the considered FD-relay system is calculated by

$$\mathcal{C} = \mathbb{E}\Big\{\log_2(1+\gamma_{\rm e2e})\Big\} = \int_0^\infty \log_2(1+\gamma_{\rm e2e})f_{\gamma_{\rm e2e}}(\gamma)d\gamma, \tag{24}$$

where $f(.)$ is the probability density function (PDF) of $\gamma_{\rm e2e}$.

After some mathematical transforms, (24) becomes

$$\mathcal{C} = \frac{1}{\ln 2}\int_0^\infty \frac{1-F(x)}{1+x}dx, \tag{25}$$

where $F(.)$ is the CDF of $\gamma_{\rm e2e}$.

Based on (25), the EC of the considered FD relay system is derived in the following Theorem 3.

Theorem 3. *The ergodic capacity of the considered FD relay system with I-CSI, THN, and RSI over Nakagami-m fading channels is expressed as*

$$\mathcal{C} = \frac{\pi}{G\ln 2}\sum_{g=1}^{G}\sum_{i=0}^{m_1N_{\rm S}-1}\sum_{j=0}^{m_2N_{\rm D}-1}\frac{A^iB^j}{i!j!\Big(2\Delta^2+1+\phi_g\Big)} \times \frac{\sqrt{1-\phi_g^2}\Big(1+\phi_g\Big)^{i+j}}{\Big(2\Delta^2-(1+\phi_g)k_{\rm SR}^2\Big)^i\Big(2\Delta^2-(1+\phi_g)k_{\rm RD}^2\Big)^j} \times \exp\Big(-\frac{(1+\phi_g)A}{2\Delta^2-(1+\phi_g)k_{\rm SR}^2} - \frac{(1+\phi_g)B}{2\Delta^2-(1+\phi_g)k_{\rm RD}^2}\Big). \tag{26}$$

Proof: Detailed proof is presented in Appendix C.

IV. Numerical Results and Discussions

In this section, the impacts of I-CSI, THN, and RSI on the performance of the considered FD relay system are evaluated by using the mathematical expressions of OP, SER, and EC derived in previous section. In addition, the OP, SER, and EC with all ideal factors (P-CSI, P-TH, and P-SIC) are also provided to clearly show the impacts of I-CSI, THN, and RSI. In all investigated scenarios, the parameters are chosen as: the average transmission power of S and R are $P_{\rm S} = P_{\rm R} = P$; the average channel gains of S–R and R–D links are $\Omega_{\rm SR} = \Omega_{\rm RD} = \Omega$; the Nakagami-$m$ fading parameters are $m_1 = m_2 = m$; the variances of channel estimation errors are $\sigma_{e_{\rm SR}}^2 = \sigma_{e_{\rm RD}}^2 = \sigma_e^2$; the THN levels are $k_{\rm S}^{\rm t} = k_{\rm R}^{\rm r} = k_{\rm R}^{\rm t} = k_{\rm D}^{\rm r} = k$; the variances of Gaussian noises are $\sigma_{\rm R}^2 = \sigma_{\rm D}^2 = \sigma^2$; the number of transmitting antennas at S and receiving antennas at D are $N_{\rm S} = N_{\rm D} = N$; the average SNR is computed as $\mathrm{SNR} = P/\sigma^2$. Note that the parameter settings in this section are similar to those in the literature such as [14], [15], [20], [21], [36], [37], [46]–[48]. Specifically, the variance of channel estimation error and the RSI level are from

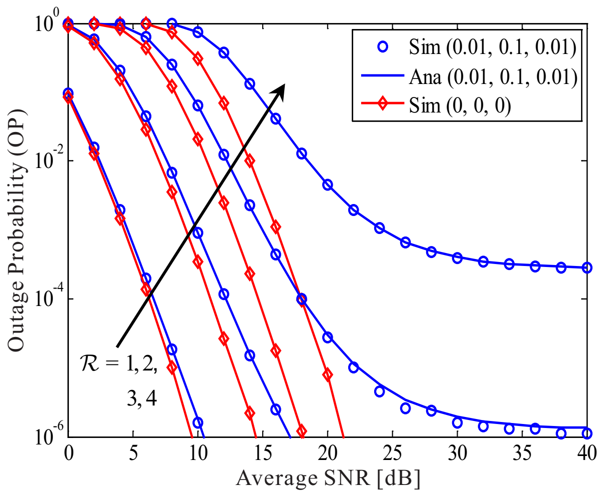

Fig. 2. The impacts of I-CSI, THN, and RSI on the OP of the considered FD relay systems for different data transmission rates, $\mathcal{R} = 1, 2, 3, 4$ bpcu; $m = 2$, $\Omega = 2$, $N = 3$, $\sigma_e^2 = 0.01$, $k = 0.1$ and $l = 0.01$.

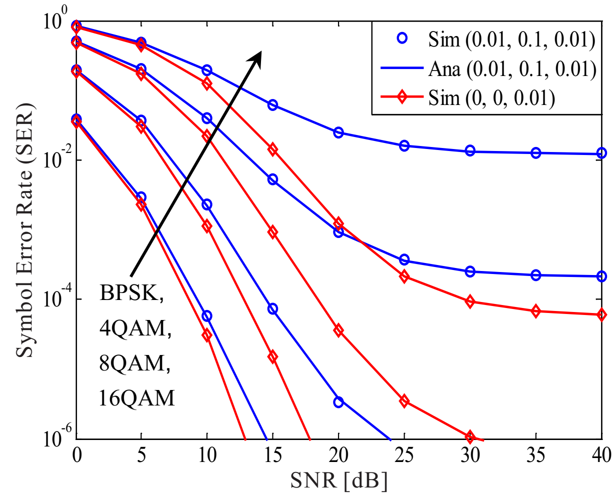

Fig. 3. The SERs of the considered FD relay system versus the average SNR for different modulation schemes.

the experiments and measurements in [14], [47], [48] and [14], [15], [36], [37], respectively. Meanwhile, the THN levels are chosen based on the experiments and measurements in [20], [21], [46]. For the sake of clarity, the parameter settings for evaluating the system performance are summarized in Table I.

TABLE I
PARAMETER SETTINGS FOR EVALUATING THE SYSTEM PERFORMANCE.

Notation	Description	Fixed value	Varying range
SNR	Signal-to-noise ratio	30 dB	$0 \sim 40$ dB
Ω	Average channel gain	2	1, 3
m	Nakagami-m fading parameter	2	1, 3
σ_e^2	Variance of channel estimation error	0.01	$0 \sim 0.2$
k	THN level	0.1	$0 \sim 0.3$
l	RSI level	0.01	$0 \sim 0.2$
$\mathcal{R}$	Minimum required data rate	1 bpcu	2, 3, 4 bit/s/Hz
(α, β)	Modulation pair	(1, 2)	$(2,1), (4-\sqrt{2}, 3/7), (3, 1/5)$

Fig. 2 investigates the impacts of I-CSI, THN, and RSI on the OP of the considered FD relay systems for different data transmission rates, i.e., $\mathcal{R} = 1, 2, 3, 4$ bpcu. In Fig. 2 and other figures, the triad $(., ., .)$ indicates (σ_e^2, k, l), i.e., $(0.01, 0.1, 0.01)$ denotes $\sigma_e^2 = 0.01$, $k = 0.1$, and $l = 0.01$. The case of all ideal factors is denoted by $(0, 0, 0)$, meaning $\sigma_e^2 = k = l = 0$. The analysis curves are plotted by using (14) while the markers represent Monte-Carlo simulation results. It is obvious that the impacts of I-CSI, THN, and RSI are remarkable for high data transmission rates. Specifically, when $\mathcal{R} = 1$ bpcu, the difference between two cases $(0.01, 0.1, 0.01)$ and $(0, 0, 0)$ is very small and can be neglected. However, for higher data transmission rates, the difference between the two cases is significant. When $\mathcal{R} = 2$ bpcu, to obtain OP $= 10^{-6}$, the case $(0.01, 0.1, 0.01)$ needs SNR = 17 dB while the case $(0, 0, 0)$ only needs SNR = 14 dB. When $\mathcal{R} = 3$ bpcu, the case $(0.01, 0.1, 0.01)$ is saturated at SNR = 40 dB with OP $\approx 10^{-6}$ while the case $(0, 0, 0)$ reaches OP $= 10^{-6}$ at SNR = 18 dB. Especially, when $\mathcal{R} = 4$ bpcu, the OP of the case $(0.01, 0.1, 0.01)$ is saturated fast at OP $= 4 \times 10^{-4}$ while the OP of the case $(0, 0, 0)$ still goes down and reaches OP $= 10^{-6}$ at SNR = 21 dB. These results demonstrate the strong impacts of I-CSI, THN, and RSI on high-rate system. As a result, the system with I-CSI, THN, and RSI is appropriate for low-rate transmission. Furthermore, when high transmission rate is used, a suitable transmission power should be chosen to save the energy of the system. For example, when $\mathcal{R} = 4$ bpcu, we should use SNR = 30 dB instead of SNR = 40 dB because the OPs of both SNRs are similar.

Fig. 3 shows the SERs of the considered FD relay system versus the average SNR for different modulation schemes, i.e., BPSK, 4QAM, 8QAM, and 16QAM corresponding to $(\alpha, \beta) = (1, 2)$, $(\alpha, \beta) = (2, 1)$, $(\alpha, \beta) = (4 - \sqrt{2}, 3/7)$, and $(\alpha, \beta) = (3, 1/5)$. We use (23) in Theorem 2 to obtain the analysis curves of SER. The parameters for obtaining Fig. 3 are similar to those used in Fig. 2. It is also noted that unlike Fig. 2, Fig. 3 compares between the SER of the considered system with I-CSI, THN, and RSI (the case $(0.01, 0.1, 0.01)$) and that of the system with P-CSI and P-TH, and I-SIC (the case of $(0, 0, 0.01)$). Like the OP, the impacts of I-CSI, THN, and RSI on the SER of the considered FD relay system are stronger in the high SNR regime. Furthermore, these impacts are significant even for BPSK modulation, i.e., the SERs in both cases $(0.01, 0.1, 0.01)$ and $(0, 0, 0.01)$ of BPSK modulation are noticeable when SNR > 10 dB. In addition, the SERs with high-order modulation schemes (8QAM and 16QAM) go to the error floor faster for both cases $(0.01, 0.1, 0.01)$ and $(0, 0, 0.01)$, especially when 16QAM is used. Although P-CSI and P-TH exist, the RSI due to I-SIC causes the error floor in the FD relay system, particularly for high order modulation schemes (refer to the case $(0, 0, 0.01)$). Therefore, more efforts

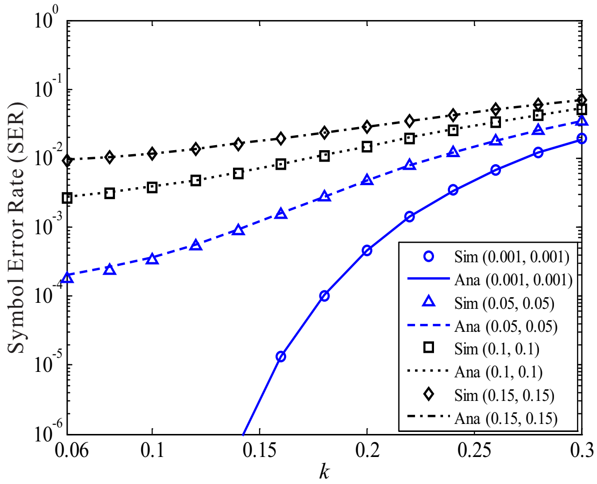

Fig. 4. The SERs of the considered FD relay system versus the level of THN k for different values of σ_e^2 and l, using 4QAM modulation, $m = 2$, $\Omega = 2$, $N = 3$.

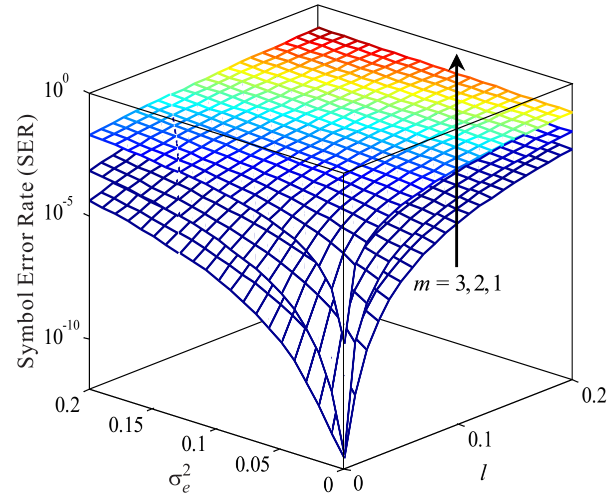

Fig. 5. The joint effect of both σ_e^2 and l on the SER of the considered FD relay systems using 4QAM modulation for different values of Nakagami-m parameter, $k = 0.1$, $\Omega = m$, and SNR = 30 dB.

to reduce the RSI level should be carried out often to decrease and avoid the error floor for SER of the considered FD relay system[7]. On the other hand, the saturation floors in high SNR regime for $\mathcal{R} = 3, 4$ bpcu are reasonable because the OP is a constant in high SNR regime as presented in (20).

Fig. 4 considers the impact of THN on the SER of the considered FD relay system using 4QAM modulation for different values of σ_e^2 and l, i.e., $\sigma_e^2 = l = 0.001, 0.05, 0.1$ and 0.15, denoted by dyad $(.,.)$. Due to the terms $1/k_{\rm SR}^2$ and $1/k_{\rm RD}^2$ in the mathematical expressions, we cannot set $k = 0$ for evaluation[8]. From Fig. 4 it is obvious that the impact of k is remarkable when σ_e^2 and l are small. Specifically, when $\sigma_e^2 = l = 0.001$, the SER rapidly changes in the range $k \in [0.06, 0.3]$. However, for higher values of σ_e^2 and l, e.g., $\sigma_e^2 = l = 0.05$, the SER slowly varies. Especially, when $\sigma_e^2 = l = 0.1$ and $\sigma_e^2 = l = 0.15$, the impact of k on the SER is slight. These features are reasonable for the considered FD relay system because when σ_e^2 and l are very small their influences can be neglected. Thus, in this case, the THN becomes the main negative factor in the considered system. When both σ_e^2 and l are larger, the impacts of them on SER become stronger than that of k. Therefore, the SER changes slowly for the wide range of k.

Fig. 5 shows the joint effect of both σ_e^2 and l on the SER of the considered FD relay systems for different values of Nakagami-m parameter, i.e., $m = 1, 2, 3$. When $m = 1$, we obtain the SER of the considered system over Rayleigh fading channels. As can be seen from Fig. 5, when $\sigma_e^2 = l = 0$, SER is the lowest because the considered system is only affected by THN. In other words, we obtain the SER of the FD relay system with P-CSI and P-SIC. In this case, this SER becomes the SER of HD relay system with THN. Specifically, SER $= 2.6 \times 10^{-12}, 3.7 \times 10^{-12}$, and 1.1×10^{-7} corresponding

[7]Notice that for the investigated parameters, the diversity order of the considered FD relay system is two. In addition, the SER performance of this system in the cases that using BPSK and 4-QAM modulation schemes satisfy the requirements of data service in cellular systems.

[8]Notice that the THN level ranges 0.08 to 0.175 in 3GPP LTE system [46].

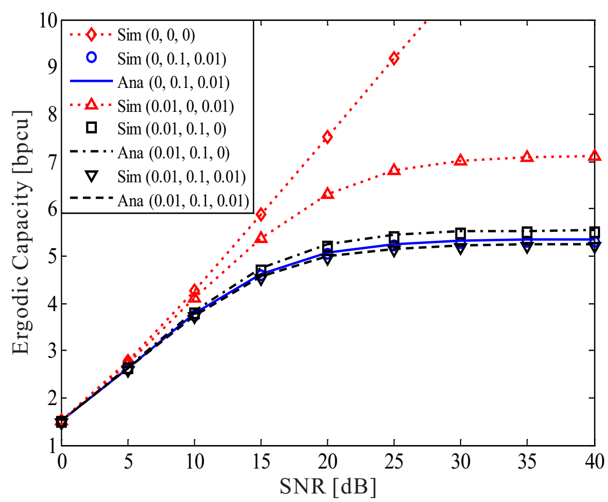

Fig. 6. The ergodic capacity of the considered FD relay system versus the average SNR for different values of σ_e^2, k, and l.

to $m = 3, 2$, and 1. When both σ_e^2 and l increase, SER rapidly increases. Particularly, when $\sigma_e^2 = l = 0.01$, SER $= 2.9 \times 10^{-9}, 3.5 \times 10^{-7}$, and 2.5×10^{-4} corresponding to $m = 3, 2$, and 1. Therefore, SER of $\sigma_e^2 = l = 0.01$ increases $10^3, 10^5$, and 10^3 times compared with that of $\sigma_e^2 = l = 0$ corresponding to $m = 3, 2$, and 1. With higher values of σ_e^2 and l, e.g., $\sigma_e^2 = l = 0.05$, SER are significantly higher, i.e., SER $= 2.2 \times 10^{-5}, 3.7 \times 10^{-4}$, and 1.1×10^{-2} corresponding to $m = 3, 2$, and 1.

Fig. 6 analyzes the EC of the considered FD relay system for different values of σ_e^2, k, and l, i.e, (σ_e^2, k, l) = (0, 0, 0), (0, 0.1, 0.01), (0.01, 0, 0.01), (0.01, 0.1, 0), and (0.01, 0.1, 0.01). The analysis curves are obtained by using (26) in Theorem 3. As can be seen from Fig. 6, in the case of all ideal factors, i.e., $(0, 0, 0)$, the EC is significantly high because the EC in this case is two times higher than that of the traditional HD relay system with P-CSI and P-TH. Among

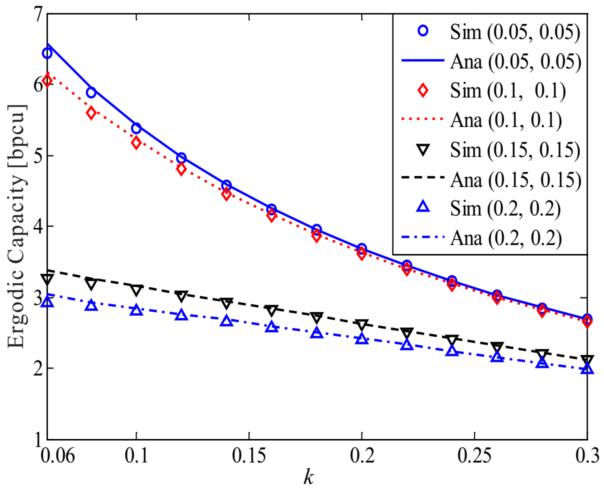

Fig. 7. The impact of THN on the EC of the considered FD relay system for some values of σ_e^2, and l, $\Omega = 2$, $m = 2$, SNR = 30 dB.

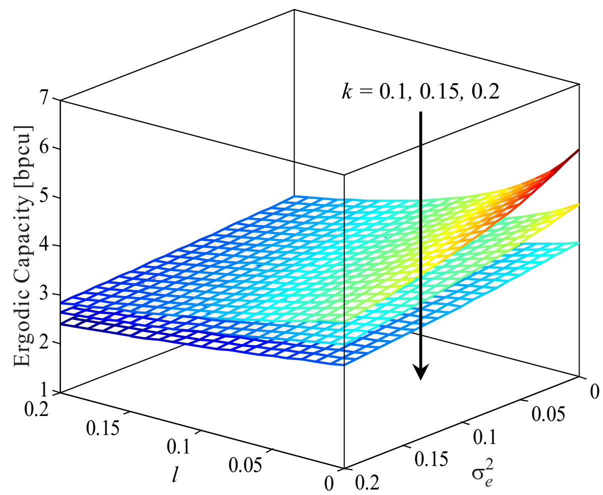

Fig. 8. The EC of the considered FD relay system under the joint impact of I-CSI and RSI for three values of k, $\Omega = 2$, $m = 2$, SNR = 30 dB.

the remaining cases, the EC of (0.01, 0, 0.01) is the best. The ECs of (0, 0.1, 0.01), (0.01, 0.1, 0), and (0.01, 0.1, 0.01) are nearly similar. Specifically, at SNR = 30 dB, EC = 11, 7, and 5.2 bpcu corresponding to (0, 0, 0), (0.01, 0, 0.01), and other cases, respectively. With the investigated values of σ_e^2, k, and l, the impact of k is strongest, it is because the EC of (0.01, 0, 0.01) is higher than that of (0, 0.1, 0.01), (0.01, 0.1, 0).

Fig. 7 depicts the impact of THN on the EC of the considered FD relay system for some values of σ_e^2, and l, i.e., $\sigma_e^2 = l = 0.05, 0.1, 015, 0.2$. Like the SER in Fig. 4, the EC is greatly affected by THN, especially when σ_e^2 and l are small. In the first case $\sigma_e^2 = l = 0.05$, the EC changes from 6.5 to 2.8 bpcu for the investigated range of k (from 0.06 to 0.3). In the second case $\sigma_e^2 = l = 0.1$, although both σ_e^2 and l are higher, the EC of the considered system is almost similar to the first case. Specifically, the EC changes from 6 to 2.8 bpcu in this case. However, for higher σ_e^2 and l, e.g., $\sigma_e^2 = l = 0.15$ and $\sigma_e^2 = l = 0.2$, the ECs of these two cases are different from two previous cases because the EC changes from 3 to 2 bpcu in these two cases. As a result, when both σ_e^2 and l change from 0.05 to 0.1, the SER significantly increases (refer to Fig. 4) while the EC slightly decreases (refer to Fig. 7). However, when both σ_e^2 and l change from 0.1 to 0.15, the SER slightly increases (refer to Fig. 4) while the EC significantly decreases (refer to Fig. 7). Since this is a major difference between SER and EC of the considered FD relay system, we need to investigate both SER and EC further to show the impact of THN on the system performance clearly.

Fig. 8 illustrates the EC of the considered FD relay system under the joint impact of I-CSI and RSI for three values of k, i.e., $k = 0.1, 0.15$, and 0.2. When both σ_e^2 and l change from 0 to 0.2, the ECs change from 5.7 to 2.8, from 3.8 to 2.4, and from 2.7 to 2 bpcu, corresponding to $k = 0.1, 0.15$, and 0.2. Obviously, the impact of l is stronger than that of σ_e^2 because the reduction of the EC caused by l is faster than that caused by σ_e^2. For example, the ECs of $\sigma_e^2 = 0$ and $l = 0.02$ are $5, 3.57, 2.63$ bpcu while the ECs of $\sigma_e^2 = 0.02$ and $l = 0$ are $5.37, 3.67, 2.67$ bpcu for $k = 0.1, 0.15$, and 0.2, respectively. For higher σ_e^2 and l, the EC of the considered FD relay system is strongly reduced. Therefore, besides all SIC techniques for FD transmission mode, various solutions to reduce the channel estimation error and transceiver hardware imperfection should be exploited together to improve the performance of FD relay system.

V. Conclusion

P-CSI and P-TH are not realistic for practical wireless communication systems because the characteristics of both channel and transceiver hardware are random and time-varying. Therefore, neglecting I-CSI and THN for wireless communication systems may cause an inaccurate evaluation of system performance. In this paper, we investigated the performance of an FD relay system where multiple-antennas at source and destination are exploited under realistic scenarios, including I-CSI, THN, and RSI. We successfully obtained the closed-form expressions of the OP, SER, and EC of the considered FD relay system over Nakagami-m fading channels. Numerical results indicated that three negative factors significantly impact the OP, SER, and EC of the considered system, especially when the system's data transmission rate and modulation order are high. Besides, when two of the three factors are large enough, the remaining factor's influence can be neglected. Furthermore, three negative factors caused the saturated minimal OP and SER and the saturated maximal EC. Therefore, depending on the certain values of three negative factors obtained through measurements and experiments, we can select a suitable transmission power for this system to avoid the performance limitations and save energy consumption.

Appendix A

This appendix gives the step-by-step presentation of how to obtain the OP of the considered FD relay system with I-CSI, THN, and RSI over Nakagami-m fading channels.

First, we begin from the probability density function (PDF, denoted by $f(x)$) and the cumulative distribution function

(CDF, denoted by $F(x)$) of the random instantaneous channel gain $|h|^2$ that follows Nakagami-m distribution, i.e.,

$$f_{|h|^2}(x) = \Big(\frac{m}{\Omega}\Big)^m \frac{x^{m-1}}{\Gamma(m)} \exp\Big(-\frac{mx}{\Omega}\Big), x \geqslant 0, \tag{27}$$

$$\begin{aligned} F_{|h|^2}(x) &= \frac{1}{\Gamma(m)} \gamma(m, \frac{mx}{\Omega}) \\ &= 1 - \exp\Big(-\frac{mx}{\Omega}\Big) \sum_{i=0}^{m-1} \frac{1}{i!} \Big(\frac{mx}{\Omega}\Big)^i, x \geqslant 0, \end{aligned} \tag{28}$$

where m is the Nakagami fading parameter of link h; $\Gamma(m) = (m-1)!$ and $\gamma(.,.)$ denote the Gamma function and lower incomplete Gamma function [49], respectively; $\Omega = \mathbb{E}\{|h|^2\}$ is the average channel gain of $|h|^2$.

When multiple antennas and MRT/MRC techniques are exploited, we have $N_{\rm S}$ and $N_{\rm D}$ channel gains for S–R and R–D links, respectively. In this case, the PDF and CDF of N channel gains, i.e., $\|\mathbf{h}\|^2$, are computed as [50]

$$f_{\|\mathbf{h}\|^2}(x) = \Big(\frac{m}{\Omega}\Big)^{mN} \frac{x^{mN-1}}{\Gamma(mN)} \exp\Big(-\frac{mx}{\Omega}\Big), x \geqslant 0, \tag{29}$$

$$F_{\|\mathbf{h}\|^2}(x) = 1 - \exp\Big(-\frac{mx}{\Omega}\Big) \sum_{i=0}^{mN-1} \frac{1}{i!} \Big(\frac{mx}{\Omega}\Big)^i, x \geqslant 0. \tag{30}$$

Now, we apply (27), (28), (29), and (30) to calculate the OP of the considered system.

To derive the OP expression from (13), we have to calculate two probabilities, i.e., $\Pr\{\gamma_{\rm R} < \gamma_{\rm th}\}$ and $\Pr\{\gamma_{\rm D} < \gamma_{\rm th}\}$. Firstly, the probability $\Pr\{\gamma_{\rm R} < \gamma_{\rm th}\}$ is computed as (31). To obtain the exact closed-form expression of (31), we consider two cases, i.e., $1 - \gamma_{\rm th} k_{\rm SR}^2 \leq 0$ and $1 - \gamma_{\rm th} k_{\rm SR}^2 > 0$.

For $1 - \gamma_{\rm th} k_{\rm SR}^2 \leq 0$ or $\gamma_{\rm th} \geq \frac{1}{k_{\rm SR}^2}$, we always have $\|\mathbf{h}_{\rm SR}\|^2 P_{\rm S}(1 - \gamma_{\rm th} k_{\rm SR}^2) \leq 0$ while $\gamma_{\rm th}[\sigma_{e_{\rm SR}}^2 P_{\rm S}(1 + k_{\rm SR}^2) + N_{\rm S}(l^2 P_{\rm R} + \sigma_{\rm R}^2)] > 0$. Therefore, the even on the right side of (31) always happens or $\Pr\{\gamma_{\rm R} < \gamma_{\rm th}\} = 1$.

For $1 - \gamma_{\rm th} k_{\rm SR}^2 > 0$ or $\gamma_{\rm th} < \frac{1}{k_{\rm SR}^2}$, the probability in (31) can be rewritten as (32). Applying (30), (32) becomes (33). Combining the two above cases, the probability of $\Pr\{\gamma_{\rm R} < \gamma_{\rm th}\}$ is given by (34). Similarly, the probability of $\Pr\{\gamma_{\rm D} < \gamma_{\rm th}\}$ is provided in (35). Substituting (34) and (35) into (13), we get the exact closed-form expression of the OP of the considered FD relay system as in Theorem (1). The proof is thus complete.

Appendix B

This appendix presents the detailed calculation of the SERs of the considered FD relay system.

As seen from (22), SER is calculated from CDF, $F(x)$, of the end-to-end SINDR. The CDF, $F(x)$ is computed as

$$F_{\gamma_{\rm e2e}}(x) = \Pr\{\gamma_{\rm e2e} < x\}. \tag{36}$$

Based on (12) and (36), it is obvious that we can obtain $F(x)$ from OP by replacing $\gamma_{\rm th}$ by x. As a result, the $F(x)$ is given by (37).

Now, SER from (22) becomes (38). The first integral in (38) can be easily solved by applying [49, Eq. (3.361.2)], i.e.,

$$\int_0^\infty \frac{\exp\Big(-\frac{x\beta}{2}\Big)}{\sqrt{x}} dx = \sqrt{\frac{2\pi}{\beta}}. \tag{39}$$

The second integral in (38) can be solved by using [51, Eq. (25.4.30)] to obtain (40), where G and Φ_g are defined as in Theorem 2.

Substituting (39) and (40) into (38) and applying some simple transforms, we obtain the SER as given in (23) of Theorem 2. The proof is thus complete.

Appendix C

This appendix provides the detailed derivations of the EC of the considered FD relay system under the impacts of I-CSI, THN, and RSI over Nakagami-m fading channels.

Replacing $F(x)$ in (37) into (25), we obtain (41). Applying [51, Eq. (25.4.30)], the integral in (41) can be calculated as (42). Substituting (42) into (41) and applying some mathematical transformations, we obtain the EC of the considered system as in Theorem 3. The proof is complete.

References

[1] A. H. Gazestani, S. A. Ghorashi, B. Mousavinasab, and M. Shikh-Bahaei, "A survey on implementation and applications of full duplex wireless communications," *Phys. Commun.*, vol. 34, pp. 121–134, 2019.

[2] K. A. Darabkh, O. M. Amro, H. B. Salameh, and R. T. Al-Zubi, "A-Z overview of the in-band full-duplex cognitive radio networks," *Comput. Commun.*, vol. 145, pp. 66–95, 2019.

[3] Q. Si, M. Jin, Y. Chen, N. Zhao, and X. Wang, "Performance analysis of spatial modulation aided NOMA with full-duplex relay," *IEEE Trans. Veh. Technol.*, vol. 69, no. 5, pp. 5683–5687, 2020.

[4] B. C. Nguyen, X. N. Tran, D. T. Tran, X. N. Pham, and L. T. Dung, "Impact of hardware impairments on the outage probability and ergodic capacity of one-way and two-way full-duplex relaying systems," *IEEE Trans. Veh. Technol.*, vol. 69, no. 8, pp. 8555–8567, 2020.

[5] L. V. Nguyen, B. C. Nguyen, X. N. Tran, and L. T. Dung, "Transmit antenna selection for full-duplex spatial modulation multiple-input multiple-output system," *IEEE Syst. J.*, vol. 14, no. 4, pp. 4777–4785, 2020.

[6] B. C. Nguyen, T. N. Kieu, T. M. Hoang, P. T. Tran, and M. Voznák, "Analysis of MRT/MRC diversity techniques to enhance the detection performance for MIMO signals in full-duplex wireless relay networks with transceiver hardware impairment," *Phys. Commun.*, vol. 42, p. 101132, 2020.

[7] G. Liu, F. R. Yu, H. Ji, V. C. M. Leung, and X. Li, "In-band full-duplex relaying: A survey, research issues and challenges," *IEEE Commun. Surv. Tutorials*, vol. 17, no. 2, pp. 500–524, 2015.

[8] G. Chen, P. Xiao, J. R. Kelly, B. Li, and R. Tafazolli, "Full-duplex wireless-powered relay in two way cooperative networks," *IEEE Access*, vol. 5, pp. 1548–1558, 2017.

[9] S. Narayanan, H. Ahmadi, and M. F. Flanagan, "On the performance of spatial modulation MIMO for full-duplex relay networks," *IEEE Trans. Wirel. Commun.*, vol. 16, no. 6, pp. 3727–3746, 2017.

[10] C. Li, B. Xia, S. Shao, Z. Chen, and Y. Tang, "Multi-user scheduling of the full-duplex enabled two-way relay systems," *IEEE Trans. Wirel. Commun.*, vol. 16, no. 2, pp. 1094–1106, 2017.

[11] G. J. González, F. H. Gregorio, J. E. Cousseau, T. Riihonen, and R. Wichman, "Full-duplex amplify-and-forward relays with optimized transmission power under imperfect transceiver electronics," *EURASIP J. Wirel. Commun. Netw.*, vol. 2017, p. 76, 2017.

[12] B. C. Nguyen, X. N. Tran, D. T. Tran, and L. T. Dung, "Full-duplex amplify-and-forward relay system with direct link: Performance analysis and optimization," *Phys. Commun.*, vol. 37, p. 100888, 2019.

[13] L. V. Nguyen, B. C. Nguyen, X. N. Tran, and L. T. Dung, "Closed-form expression for the symbol error probability in full-duplex spatial modulation relay system and its application in optimal power allocation," *Sensors*, vol. 19, no. 24, p. 5390, 2019.

$$\begin{aligned}\Pr\{\gamma_{\mathrm{R}} < \gamma_{\mathrm{th}}\} &= \Pr\{\frac{\|\mathbf{h}_{\mathrm{SR}}\|^2 P_{\mathrm{S}}}{\|\mathbf{h}_{\mathrm{SR}}\|^2 k_{\mathrm{SR}}^2 P_{\mathrm{S}} + \sigma_{e_{\mathrm{SR}}}^2 P_{\mathrm{S}}(1+k_{\mathrm{SR}}^2) + N_{\mathrm{S}}(l^2 P_{\mathrm{R}} + \sigma_{\mathrm{R}}^2)} < \gamma_{\mathrm{th}}\} \\ &= \Pr\{\|\mathbf{h}_{\mathrm{SR}}\|^2 P_{\mathrm{S}}(1-\gamma_{\mathrm{th}} k_{\mathrm{SR}}^2) < \gamma_{\mathrm{th}}[\sigma_{e_{\mathrm{SR}}}^2 P_{\mathrm{S}}(1+k_{\mathrm{SR}}^2) + N_{\mathrm{S}}(l^2 P_{\mathrm{R}} + \sigma_{\mathrm{R}}^2)]\}.\end{aligned} \tag{31}$$

$$\Pr\{\gamma_{\mathrm{R}} < \gamma_{\mathrm{th}}\} = \Pr\left\{\|\mathbf{h}_{\mathrm{SR}}\|^2 < \frac{\gamma_{\mathrm{th}}[\sigma_{e_{\mathrm{SR}}}^2 P_{\mathrm{S}}(1+k_{\mathrm{SR}}^2) + N_{\mathrm{S}}(l^2 P_{\mathrm{R}} + \sigma_{\mathrm{R}}^2)]}{P_{\mathrm{S}}(1-\gamma_{\mathrm{th}} k_{\mathrm{SR}}^2)}\right\}. \tag{32}$$

$$\begin{aligned}\Pr\{\gamma_{\mathrm{R}} < \gamma_{\mathrm{th}}\} =& 1 - \exp\left(-\frac{\gamma_{\mathrm{th}} m_1[\sigma_{e_{\mathrm{SR}}}^2 P_{\mathrm{S}}(1+k_{\mathrm{SR}}^2) + N_{\mathrm{S}}(l^2 P_{\mathrm{R}} + \sigma_{\mathrm{R}}^2)]}{(1-\gamma_{\mathrm{th}} k_{\mathrm{SR}}^2)\Omega_{\mathrm{SR}} P_{\mathrm{S}}}\right) \\ &\times \sum_{i=0}^{m_1 N_{\mathrm{S}}-1} \frac{1}{i!}\left(\frac{\gamma_{\mathrm{th}} m_1[\sigma_{e_{\mathrm{SR}}}^2 P_{\mathrm{S}}(1+k_{\mathrm{SR}}^2) + N_{\mathrm{S}}(l^2 P_{\mathrm{R}} + \sigma_{\mathrm{R}}^2)]}{(1-\gamma_{\mathrm{th}} k_{\mathrm{SR}}^2)\Omega_{\mathrm{SR}} P_{\mathrm{S}}}\right)^i \\ =& 1 - \exp\left(-\frac{\gamma_{\mathrm{th}} A}{1-\gamma_{\mathrm{th}} k_{\mathrm{SR}}^2}\right)\sum_{i=0}^{m_1 N_{\mathrm{S}}-1} \frac{1}{i!}\left(\frac{\gamma_{\mathrm{th}} A}{1-\gamma_{\mathrm{th}} k_{\mathrm{SR}}^2}\right)^i.\end{aligned} \tag{33}$$

$$\Pr\{\gamma_{\mathrm{R}} < \gamma_{\mathrm{th}}\} = \begin{cases} 1 - \exp\left(-\frac{\gamma_{\mathrm{th}} A}{1-\gamma_{\mathrm{th}} k_{\mathrm{SR}}^2}\right)\sum_{i=0}^{m N_{\mathrm{S}}-1} \frac{1}{i!}\left(\frac{\gamma_{\mathrm{th}} A}{1-\gamma_{\mathrm{th}} k_{\mathrm{SR}}^2}\right)^i, & \gamma_{\mathrm{th}} < \frac{1}{k_{\mathrm{SR}}^2}, \\ 1, & \gamma_{\mathrm{th}} \geq \frac{1}{k_{\mathrm{SR}}^2}. \end{cases} \tag{34}$$

[14] D. Choi and J. H. Lee, "Outage probability of two-way full-duplex relaying with imperfect channel state information," *IEEE Commun. Lett.*, vol. 18, no. 6, pp. 933–936, 2014.

[15] C. Li, H. Wang, Y. Yao, Z. Chen, X. Li, and S. Zhang, "Outage performance of the full-duplex two-way DF relay system under imperfect CSI," *IEEE Access*, vol. 5, pp. 5425–5435, 2017.

[16] H. Iimori, G. T. F. de Abreu, and G. C. Alexandropoulos, "MIMO beamforming schemes for hybrid SIC FD radios with imperfect hardware and CSI," *IEEE Trans. Wirel. Commun.*, vol. 18, no. 10, pp. 4816–4830, 2019.

[17] A. V. and A. V. Babu, "Full/half duplex cooperative NOMA under imperfect successive interference cancellation and channel state estimation errors," *IEEE Access*, vol. 7, pp. 179 961–179 984, 2019.

[18] X. Li, W. Wang, M. Zhang, F. Zhou, and N. Al-Dhahir, "Robust secure beamforming for SWIPT-aided relay systems with full-duplex receiver and imperfect CSI," *IEEE Trans. Veh. Technol.*, vol. 69, no. 2, pp. 1867–1878, 2020.

[19] H. Iimori, G. T. F. de Abreu, and K. Ishibashi, "Full-duplex MIMO systems with hardware limitations and imperfect channel estimation," in *IEEE Global Communications Conference, GLOBECOM 2020, Virtual Event, Taiwan, December 7-11, 2020*. IEEE, 2020, pp. 1–6.

[20] T. Schenk, *RF imperfections in high-rate wireless systems: impact and digital compensation*. Springer Science & Business Media, 2008.

[21] E. Björnson, J. Hoydis, M. Kountouris, and M. Debbah, "Massive MIMO systems with non-ideal hardware: Energy efficiency, estimation, and capacity limits," *IEEE Trans. Inf. Theory*, vol. 60, no. 11, pp. 7112–7139, 2014.

[22] A. K. Papazafeiropoulos, S. K. Sharma, T. Ratnarajah, and S. Chatzinotas, "Impact of residual additive transceiver hardware impairments on rayleigh-product MIMO channels with linear receivers: Exact and asymptotic analyses," *IEEE Trans. Commun.*, vol. 66, no. 1, pp. 105–118, 2018.

[23] S. Solanki, P. K. Upadhyay, D. B. da Costa, P. S. Bithas, A. G. Kanatas, and U. S. Dias, "Joint impact of RF hardware impairments and channel estimation errors in spectrum sharing multiple-relay networks," *IEEE Trans. Commun.*, vol. 66, no. 9, pp. 3809–3824, 2018.

[24] S. Solanki, P. K. Upadhyay, D. B. da Costa, P. S. Bithas, and A. G. Kanatas, "Performance analysis of cognitive relay networks with RF hardware impairments and CEEs in the presence of primary users' interference," *IEEE Trans. Cogn. Commun. Netw.*, vol. 4, no. 2, pp. 406–421, 2018.

[25] X. Li, J. Li, P. T. Mathiopoulos, D. Zhang, L. Li, and J. Jin, "Joint impact of hardware impairments and imperfect CSI on cooperative SWIPT NOMA multi-relaying systems," in *IEEE/CIC International Conference on Communications in China, ICCC 2018, Beijing, China, August 16-18, 2018*. IEEE, 2018, pp. 95–99.

[26] X. Li, M. Liu, C. Deng, P. T. Mathiopoulos, Z. Ding, and Y. Liu, "Full-duplex cooperative NOMA relaying systems with I/Q imbalance and imperfect SIC," *IEEE Wirel. Commun. Lett.*, vol. 9, no. 1, pp. 17–20, 2020.

[27] C. Deng, M. Liu, X. Li, and Y. Liu, "Hardware impairments aware full-duplex NOMA networks over Rician fading channels," *IEEE Syst. J.*, pp. 1–4, 2020.

[28] V. Radhakrishnan, O. Taghizadeh, and R. Mathar, "Hardware impairments-aware transceiver design for multi-carrier full-duplex MIMO relaying," *IEEE Trans. Veh. Technol.*, vol. 70, no. 2, pp. 1109–1121, 2021.

[29] D. N. Amudala, E. Sharma, and R. Budhiraja, "Energy-efficient spatially-correlated hardware impaired massive MIMO FD relaying," *IEEE Trans. Commun.*, vol. 69, no. 3, pp. 2028–2046, 2021.

[30] F. S. Tabataba, P. Sadeghi, C. Hucher, and M. R. Pakravan, "Impact of channel estimation errors and power allocation on analog network coding and routing in two-way relaying," *IEEE Trans. Veh. Technol.*, vol. 61, no. 7, pp. 3223–3239, 2012.

[31] A. S. Ibrahim and K. J. R. Liu, "Mitigating channel estimation error with timing synchronization tradeoff in cooperative communications," *IEEE Trans. Signal Process.*, vol. 58, no. 1, pp. 337–348, 2010.

[32] E. Ahmed and A. M. Eltawil, "All-digital self-interference cancellation technique for full-duplex systems," *IEEE Trans. Wirel. Commun.*, vol. 14, no. 7, pp. 3519–3532, 2015.

[33] A. Sabharwal, P. Schniter, D. Guo, D. W. Bliss, S. Rangarajan, and R. Wichman, "In-band full-duplex wireless: Challenges and opportunities," *IEEE J. Sel. Areas Commun.*, vol. 32, no. 9, pp. 1637–1652, 2014.

[34] E. Everett, A. Sahai, and A. Sabharwal, "Passive self-interference suppression for full-duplex infrastructure nodes," *IEEE Trans. Wirel. Commun.*, vol. 13, no. 2, pp. 680–694, 2014.

$$\begin{aligned}\Pr\{\gamma_{\rm D} < \gamma_{\rm th}\} &= \Pr\left\{\frac{\|\mathbf{h}_{\rm RD}\|^2 P_{\rm R}}{\|\mathbf{h}_{\rm RD}\|^2 k_{\rm RD}^2 P_{\rm R} + \sigma_{e_{\rm SR}}^2 P_{\rm R}(1+k_{\rm RD}^2) + \sigma_{\rm D}^2} < \gamma_{\rm th}\right\} \\ &= \begin{cases} 1 - \exp\left(-\frac{\gamma_{\rm th} B}{1-\gamma_{\rm th} k_{\rm RD}^2}\right) \sum\limits_{j=0}^{m_2 N_{\rm D}-1} \frac{1}{j!}\left(\frac{\gamma_{\rm th} B}{1-\gamma_{\rm th} k_{\rm RD}^2}\right)^j, & \gamma_{\rm th} < \frac{1}{k_{\rm RD}^2}, \\ 1, & \gamma_{\rm th} \geq \frac{1}{k_{\rm RD}^2}. \end{cases}\end{aligned} \tag{35}$$

$$F(x) = \begin{cases} 1 - \exp\left(-\frac{xA}{1-xk_{\rm SR}^2} - \frac{xB}{1-xk_{\rm RD}^2}\right) \sum\limits_{i=0}^{m_1 N_{\rm S}-1} \sum\limits_{j=0}^{m_2 N_{\rm D}-1} \frac{1}{i!j!}\left(\frac{xA}{1-xk_{\rm SR}^2}\right)^i \left(\frac{xB}{1-xk_{\rm RD}^2}\right)^j, & x < 1/\Delta^2, \\ 1, & x \geq 1/\Delta^2. \end{cases} \tag{37}$$

$$\begin{aligned}\text{SER} =& \frac{\alpha\sqrt{\beta}}{2\sqrt{2\pi}}\Bigg[\int_0^{1/\Delta^2} \frac{\exp\left(-\frac{x\beta}{2}\right)}{\sqrt{x}}\Bigg(1 - \exp\left(-\frac{xA}{1-xk_{\rm SR}^2} - \frac{xB}{1-xk_{\rm RD}^2}\right) \\ & \sum_{i=0}^{m_1 N_{\rm S}-1} \sum_{j=0}^{m_2 N_{\rm D}-1} \frac{1}{i!j!}\left(\frac{xA}{1-xk_{\rm SR}^2}\right)^i \left(\frac{xB}{1-xk_{\rm RD}^2}\right)^j\Bigg) dx + \int_{1/\Delta^2}^{\infty} \frac{\exp\left(-\frac{x\beta}{2}\right)}{\sqrt{x}} dx\Bigg] \\ =& \frac{\alpha\sqrt{\beta}}{2\sqrt{2\pi}}\Bigg[\int_0^{\infty} \frac{\exp\left(-\frac{x\beta}{2}\right)}{\sqrt{x}} dx - \int_0^{1/\Delta^2} \exp\left(-\frac{xA}{1-xk_{\rm SR}^2} - \frac{xB}{1-xk_{\rm RD}^2} - \frac{x\beta}{2}\right) \\ & \sum_{i=0}^{m_1 N_{\rm S}-1} \sum_{j=0}^{m_2 N_{\rm D}-1} \frac{A^i B^j x^{i+j-\frac{1}{2}}}{i!j!(1-xk_{\rm SR}^2)^i (1-xk_{\rm RD}^2)^j} dx\Bigg].\end{aligned} \tag{38}$$

[35] T. Riihonen, S. Werner, and R. Wichman, "Mitigation of loopback self-interference in full-duplex MIMO relays," *IEEE Trans. Signal Process.*, vol. 59, no. 12, pp. 5983–5993, 2011.

[36] C. Li, Z. Chen, Y. Wang, Y. Yao, and B. Xia, "Outage analysis of the full-duplex decode-and-forward two-way relay system," *IEEE Trans. Veh. Technol.*, vol. 66, no. 5, pp. 4073–4086, 2017.

[37] D. Bharadia, E. McMilin, and S. Katti, "Full duplex radios," in *ACM SIGCOMM 2013 Conference, SIGCOMM 2013, Hong Kong, August 12-16, 2013*, D. M. Chiu, J. Wang, P. Barford, and S. Seshan, Eds. ACM, 2013, pp. 375–386.

[38] R. Vaughan, N. Scott, and D. White, "Eight hints for making and interpreting evm measurements," *Agilent Application Note*, pp. 1–12, 2005.

[39] G. Liu, X. Chen, Z. Ding, Z. Ma, and F. R. Yu, "Hybrid half-duplex/full-duplex cooperative non-orthogonal multiple access with transmit power adaptation," *IEEE Trans. Wirel. Commun.*, vol. 17, no. 1, pp. 506–519, 2018.

[40] S. Wang and T. Wu, "Stochastic geometric performance analyses for the cooperative NOMA with the full-duplex energy harvesting relaying," *IEEE Trans. Veh. Technol.*, vol. 68, no. 5, pp. 4894–4905, 2019.

[41] Y. Alsaba, C. Y. Leow, and S. K. A. Rahim, "Full-duplex cooperative non-orthogonal multiple access with beamforming and energy harvesting," *IEEE Access*, vol. 6, pp. 19 726–19 738, 2018.

[42] D. Kim, S. Park, H. Ju, and D. Hong, "Transmission capacity of full-duplex-based two-way ad hoc networks with ARQ protocol," *IEEE Trans. Veh. Technol.*, vol. 63, no. 7, pp. 3167–3183, 2014.

[43] E. Björnson, M. Matthaiou, and M. Debbah, "A new look at dual-hop relaying: Performance limits with hardware impairments," *IEEE Trans. Commun.*, vol. 61, no. 11, pp. 4512–4525, 2013.

[44] M. A. Ahmed, C. C. Tsimenidis, and A. F. Alrawi, "Performance analysis of full-duplex-MRC-MIMO with self-interference cancellation using null-space-projection," *IEEE Trans. Signal Process.*, vol. 64, no. 12, pp. 3093–3105, 2016.

[45] A. Goldsmith, *Wireless Communications*. Cambridge University Press, 2005.

[46] H. Holma and A. Toskala, *LTE for UMTS.: Evolution to LTE-Advanced*. John Wiley & Sons, 2011.

[47] A. Hyadi, M. Benjillali, and M. Alouini, "Outage performance of decode-and-forward in two-way relaying with outdated CSI," *IEEE Trans. Veh. Technol.*, vol. 64, no. 12, pp. 5940–5947, 2015.

[48] A. Tukmanov, S. Boussakta, Z. Ding, and A. Jamalipour, "Outage performance analysis of imperfect-CSI-based selection cooperation in random networks," *IEEE Trans. Commun.*, vol. 62, no. 8, pp. 2747–2757, 2014.

[49] A. Jeffrey and D. Zwillinger, *Table of integrals, series, and products*. Academic press, 2007.

[50] A. Yilmaz and O. Kucur, "Performance of transmit antenna selection and maximal-ratio combining in dual hop amplify-and-forward relay network over nakagami-m fading channels," *Wirel. Pers. Commun.*, vol. 67, no. 3, pp. 485–503, 2012.

[51] M. Abramowitz and I. A. Stegun, *Handbook of mathematical functions with formulas, graphs, and mathematical tables*. Dover, New York, 1972, vol. 9.

Ba Cao Nguyen received the B.S. degree in 2006 from Telecommunications University, Nha Trang, Vietnam, and the M.S. degree in 2011 from the Posts and Telecommunications Institute of Technology (VNPT), Ho Chi Minh City, Vietnam. He received the Ph.D. degree from Le Quy Don Technical University, Hanoi, Vietnam. He is currently a Lecturer with Telecommunications University, Nhatrang, Vietnam. His research interests include energy harvesting, full-duplex, spatial modulation, NOMA, MIMO, and cooperative communication.

$$
\begin{aligned}
&\int_0^{1/\Delta^2} \exp\Big(-\frac{xA}{1-xk_{\mathrm{SR}}^2}-\frac{xB}{1-xk_{\mathrm{RD}}^2}-\frac{x\beta}{2}\Big)\sum_{i=0}^{m_1N_{\mathrm{S}}-1}\sum_{j=0}^{m_2N_{\mathrm{D}}-1}\frac{A^iB^jx^{i+j-\frac{1}{2}}}{i!j!(1-xk_{\mathrm{SR}}^2)^i(1-xk_{\mathrm{RD}}^2)^j}dx\\
&=\sum_{i=0}^{m_1N_{\mathrm{S}}-1}\sum_{j=0}^{m_2N_{\mathrm{D}}-1}\frac{A^iB^j}{i!j!}\int_0^{1/\Delta^2}\frac{x^{i+j-\frac{1}{2}}}{(1-xk_{\mathrm{SR}}^2)^i(1-xk_{\mathrm{RD}}^2)^j}\exp\Big(-\frac{xA}{1-xk_{\mathrm{SR}}^2}-\frac{xB}{1-xk_{\mathrm{RD}}^2}-\frac{x\beta}{2}\Big)dx\\
&=\sum_{i=0}^{m_1N_{\mathrm{S}}-1}\sum_{j=0}^{m_2N_{\mathrm{D}}-1}\frac{A^iB^j\pi}{i!j!2G\Delta^2}\sum_{g=1}^{G}\frac{\Big(\frac{1+\phi_g}{2\Delta^2}\Big)^{i+j-\frac{1}{2}}\sqrt{1-\phi_g^2}}{\Big(1-\Big(\frac{1+\phi_g}{2\Delta^2}\Big)k_{\mathrm{SR}}^2\Big)^i\Big(1-\Big(\frac{1+\phi_g}{2\Delta^2}\Big)k_{\mathrm{RD}}^2\Big)^j}\\
&\qquad\qquad\times\exp\Bigg(-\frac{\Big(\frac{1+\phi_g}{2\Delta^2}\Big)A}{1-\Big(\frac{1+\phi_g}{2\Delta^2}\Big)k_{\mathrm{SR}}^2}-\frac{\Big(\frac{1+\phi_g}{2\Delta^2}\Big)B}{1-\Big(\frac{1+\phi_g}{2\Delta^2}\Big)k_{\mathrm{RD}}^2}\Bigg).
\end{aligned}
\tag{40}
$$

$$
\begin{aligned}
\mathcal{C}=&\frac{1}{\ln 2}\int_0^{1/\Delta^2}\frac{\exp\Big(-\frac{xA}{1-xk_{\mathrm{SR}}^2}-\frac{xB}{1-xk_{\mathrm{RD}}^2}\Big)\sum_{i=0}^{m_1N_{\mathrm{S}}-1}\sum_{j=0}^{m_2N_{\mathrm{D}}-1}\frac{1}{i!j!}\Big(\frac{xA}{1-xk_{\mathrm{SR}}^2}\Big)^i\Big(\frac{xB}{1-xk_{\mathrm{RD}}^2}\Big)^j}{1+x}dx\\
=&\frac{1}{\ln 2}\sum_{i=0}^{m_1N_{\mathrm{S}}-1}\sum_{j=0}^{m_2N_{\mathrm{D}}-1}\frac{A^iB^j}{i!j!}\int_0^{1/\Delta^2}\frac{x^{i+j}}{(1+x)(1-xk_{\mathrm{SR}}^2)^i(1-xk_{\mathrm{RD}}^2)^j}\exp\Big(-\frac{xA}{1-xk_{\mathrm{SR}}^2}-\frac{xB}{1-xk_{\mathrm{RD}}^2}\Big).
\end{aligned}
\tag{41}
$$

$$
\begin{aligned}
&\int_0^{1/\Delta^2}\frac{x^{i+j}}{(1+x)(1-xk_{\mathrm{SR}}^2)^i(1-xk_{\mathrm{RD}}^2)^j}\exp\Big(-\frac{xA}{1-xk_{\mathrm{SR}}^2}-\frac{xB}{1-xk_{\mathrm{RD}}^2}\Big)\\
&=\frac{\pi}{2G\Delta^2}\sum_{g=1}^{G}\frac{\sqrt{1-\phi_g^2}\Big(\frac{1+\phi_g}{2\Delta^2}\Big)^{i+j}}{\Big(1+\frac{1+\phi_g}{2\Delta^2}\Big)\Big(1-\frac{1+\phi_g}{2\Delta^2}k_{\mathrm{SR}}^2\Big)^i\Big(1-\frac{1+\phi_g}{2\Delta^2}k_{\mathrm{RD}}^2\Big)^j}\exp\Bigg(-\frac{\frac{1+\phi_g}{2\Delta^2}A}{1-\frac{1+\phi_g}{2\Delta^2}k_{\mathrm{SR}}^2}-\frac{\frac{1+\phi_g}{2\Delta^2}B}{1-\frac{1+\phi_g}{2\Delta^2}k_{\mathrm{RD}}^2}\Bigg).
\end{aligned}
\tag{42}
$$

Le The Dung (S'14–M'16) received the B.S. degree in electronics and telecommunication engineering from Ho Chi Minh City University of Technology, Ho Chi Minh City, Vietnam, in 2008, and both the M.S. and Ph.D. degrees in electronics and computer engineering from Hongik University, Seoul, South Korea, in 2012 and 2016, respectively. From 2007 to 2010, he joined Signet Design Solutions Vietnam as a Hardware Design Engineer. He has been with Chungbuk National University as a Postdoctoral Research Fellow from May 2016. He has more than 60 papers in referred international journals and conferences. His major research interests include routing protocols, network coding, network stability analysis and optimization in mobile ad-hoc networks, cognitive radio ad-hoc networks, and visible light communication networks. He was a recipient of the IEEE IS3C2016 Best Paper Award.

Tran Manh Hoang received the B.S. degree in communication command from Telecommunications University, Ministry of Defense, Nha Trang, Vietnam, in 2002, the B.Eng. degree in electrical engineering from Le Quy Don Technical University, Ha Noi, Vietnam, in 2006 the M.Eng. degree in electronics engineering from Posts and Telecommunications Institute of Technology, Ho Chi Minh City, Vietnam, in 2013 and the Ph.D degree from Le Quy Don Technical University, Hanoi, Vietnam, in 2018. He is currently a Lecturer with Telecommunications University, Nhatrang, Vietnam. His research interests include energy harvesting, non-orthogonal multiple access, and signal processing for wireless cooperative communications.

Xuan Nam Tran (M'03) is currently a full professor and head of a strong research group on advanced wireless communications, Le Quy Don Technical University. He received his Master of Engineering (ME) in Telecommunications Engineering from University of Technology Sydney, Australia in 1998, and Doctor of Engineering in Electronic Engineering from The University of Electro-Communications, Japan in 2003. From November 2003 to March 2006 he was a research associate at the Information and Communication Systems Group, Department of Information and Communication Engineering, The University of Electro-Communications, Tokyo, Japan. His research interests are in the areas of space-time signal processing for communications such as adaptive antennas, space-time coding, MIMO, spatial modulation and cooperative communications. Prof. Tran was a recipient of the 2003 IEEE AP-S Japan Chapter Young Engineer Award, and a co-recipient of two best papers from The 2012 International Conference on Advanced Technologies for Communications and The 2014 National Conference on Electronics, Communications and Information Technology. Prof. Tran is the founding chair and currently the chapter chair of the Vietnam Chapter of IEEE Communications Society. He is a member of IEEE, IEICE and the Radio-Electronics Association of Vietnam (REV).

Taejoon Kim (S'07–M'13) received his B.S. in Electronics Engineering from Yonsei University, Seoul, Republic of Korea, in 2003, and his PhD in Electrical Engineering from the Korea Advanced Institute of Science and Technology (KAIST), Daejeon, Republic of Korea, in 2011. He is currently an associate professor with the School of Information and Communication Engineering, Chungbuk National University, Chungju, Republic of Korea. From 2003 to 2005, he was a researcher with LG Electronics, Seoul, Republic of Korea. From 2011 to 2013, he was a senior researcher with Electronics and Telecommunications Research Institute (ETRI), Daejeon, Republic of Korea. His research areas include communication theory and analysis, and optimization of wireless networks.